Taken together, these data explain why NC is not readily displaced by A3G.

A major issue in research on A3G's antiviral effect is the question of whether this activity is deaminase-dependent or -independent (or both), but there is still no clear consensus. There are data favoring the dependent mechanism, as shown in several studies of G to A hypermutation (3,4,6) and in some reports on reverse transcription in Δ*vif* HIV-1-infected cells (15,37). However, there is also accumulating evidence indicating that both types of mechanisms might be involved in A3G's effect on reverse transcription *in vivo* (13,15). Our studies do not exclude a requirement for editing, but based on biochemical and biophysical analysis, provide support for a novel molecular mechanism that could account for deaminase-independent inhibition of reverse transcription and virus replication that is observed *in vivo*.

In summary, our findings demonstrate for the first time that A3G can inhibit RT-catalyzed elongation in a deaminase-independent manner without interfering with NC-mediated chaperone activity. These results suggest that A3G has an intrinsic effect on viral DNA synthesis, which is independent of the replication steps following reverse transcription. Interplay of the equilibrium and kinetic differences between HIV-1 NC, A3G and RT with respect to their nucleic acid binding interactions is likely to be a major determinant of deaminase-independent A3G inhibition of RT-catalyzed DNA extension.

SUPPLEMENTARY DATA

Supplementary Data are available at NAR online.

ACKNOWLEDGEMENTS

We thank Dr Robert J. Gorelick for his generous gift of recombinant NC protein and Dr Alan Rein for valuable discussion and critical reading of the manuscript. This research was supported in part by the Intramural Research Program of the NIH, National Institute of Child Health and Human Development (J.G.L.), the NIH Intramural AIDS Targeted Antiviral Program (A.M.G.), an NIH Kirschstein-NRSA Individual Fellowship, F32 GM072396 (K.S.M.), NIH grant GM065056 (K.M.F.), and NSF MCB-0238190 and NIH GM072462 grants (M.C.W.). Funding to pay the Open Access publication charges for the article was provided by the Intramural Research Program of the NIH, National Institute of Child Health and Human Development.

Conflict of interest statement. None declared.

REFERENCES

1. Sheehy,A.M., Gaddis,N.C., Choi,J.D. and Malim,M.H. (2002) Isolation of a human gene that inhibits HIV-1 infection and is suppressed by the viral Vif protein. *Nature*, **418**, 646–650.
2. Ehrlich,E.S. and Yu,X.F. (2006) Lentiviral Vif: viral hijacker of the ubiquitin-proteasome system. *Int. J. Hematol.*, **83**, 208–212.
3. Harris,R.S., Bishop,K.N., Sheehy,A.M., Craig,H.M., Petersen-Mahrt,S.K., Watt,I.N., Neuberger,M.S. and Malim,M.H. (2003) DNA deamination mediates innate immunity to retroviral infection. *Cell*, **113**, 803–809.
4. Lecossier,D., Bouchonnet,F., Clavel,F. and Hance,A.J. (2003) Hypermutation of HIV-1 DNA in the absence of the Vif protein. *Science*, **300**, 1112.
5. Mangeat,B., Turelli,P., Caron,G., Friedli,M., Perrin,L. and Trono,D. (2003) Broad antiretroviral defence by human APOBEC3G through lethal editing of nascent reverse transcripts. *Nature*, **424**, 99–103.
6. Yu,Q., König,R., Pillai,S., Chiles,K., Kearney,M., Palmer,S., Richman,D., Coffin,J.M. and Landau,N.R. (2004) Single-strand specificity of APOBEC3G accounts for minus-strand deamination of the HIV genome. *Nat. Struct. Mol. Biol.*, **11**, 435–442.
7. Shindo,K., Takaori-Kondo,A., Kobayashi,M., Abudu,A., Fukunaga,K. and Uchiyama,T. (2003) The enzymatic activity of CEM15/Apobec-3G is essential for the regulation of the infectivity of HIV-1 virion but not a sole determinant of its antiviral activity. *J. Biol. Chem.*, **278**, 44412–44416.
8. Navarro,F., Bollman,B., Chen,H., König,R., Yu,Q., Chiles,K. and Landau,N.R. (2005) Complementary function of the two catalytic domains of APOBEC3G. *Virology*, **333**, 374–386.
9. Newman,E.N., Holmes,R.K., Craig,H.M., Klein,K.C., Lingappa,J.R., Malim,M.H. and Sheehy,A.M. (2005) Antiviral function of APOBEC3G can be dissociated from cytidine deaminase activity. *Curr. Biol.*, **15**, 166–170.
10. Bishop,K.N., Holmes,R.K. and Malim,M.H. (2006) Antiviral potency of APOBEC proteins does not correlate with cytidine deamination. *J. Virol.*, **80**, 8450–8458.
11. Opi,S., Takeuchi,H., Kao,S., Khan,M.A., Miyagi,E., Goila-Gaur,R., Iwatani,Y., Levin,J.G. and Strebel,K. (2006) Monomeric APOBEC3G is catalytically active and has antiviral activity. *J. Virol.*, **80**, 4673–4682.
12. Iwatani,Y., Takeuchi,H., Strebel,K. and Levin,J.G. (2006) Biochemical activities of highly purified, catalytically active human APOBEC3G: correlation with antiviral effect. *J. Virol.*, **80**, 5992–6002.
13. Holmes,R.K., Koning,F.A., Bishop,K.N. and Malim,M.H. (2007) APOBEC3F can inhibit the accumulation of HIV-1 reverse transcription products in the absence of hypermutation. Comparisons with APOBEC3G. *J. Biol. Chem.*, **282**, 2587–2595.
14. Holmes,R.K., Malim,M.H. and Bishop,K.N. (2007) APOBEC-mediated viral restriction: not simply editing? *Trends Biochem. Sci.*, **32**, 118–128.
15. Luo,K., Wang,T., Liu,B., Tian,C., Xiao,Z., Kappes,J. and Yu,X.F. (2007) Cytidine deaminases APOBEC3G and APOBEC3F interact with human immunodeficiency virus type 1 integrase and inhibit proviral DNA formation. *J. Virol.*, **81**, 7238–7248.
16. Turelli,P., Mangeat,B., Jost,S., Vianin,S. and Trono,D. (2004) Inhibition of hepatitis B virus replication by APOBEC3G. *Science*, **303**, 1829.
17. Rosler,C., Kock,J., Kann,M., Malim,M.H., Blum,H.E., Baumert,T.F. and von Weizsacker,F. (2005) APOBEC-mediated interference with hepadnavirus production. *Hepatology*, **42**, 301–309.
18. Nguyen,D.H., Gummuluru,S. and Hu,J. (2007) Deamination-independent inhibition of hepatitis B virus reverse transcription by APOBEC3G. *J. Virol.*, **81**, 4465–4472.
19. Okeoma,C.M., Lovsin,N., Peterlin,B.M. and Ross,S.R. (2007) APOBEC3 inhibits mouse mammary tumour virus replication in vivo. *Nature*, **445**, 927–930.
20. Bogerd,H.P., Wiegand,H.L., Doehle,B.P., Lueders,K.K. and Cullen,B.R. (2006) APOBEC3A and APOBEC3B are potent inhibitors of LTR-retrotransposon function in human cells. *Nucleic Acids Res.*, **34**, 89–95.
21. Bogerd,H.P., Wiegand,H.L., Hulme,A.E., Garcia-Perez,J.L., O'Shea,K.S., Moran,J.V. and Cullen,B.R. (2006) Cellular inhibitors of long interspersed element 1 and Alu retrotransposition. *Proc. Natl Acad. Sci. USA.*, **103**, 8780–8785.
22. Chen,H., Lilley,C.E., Yu,Q., Lee,D.V., Chou,J., Narvaiza,I., Landau,N.R. and Weitzman,M.D. (2006) APOBEC3A is a potent inhibitor of adeno-associated virus and retrotransposons. *Curr. Biol.*, **16**, 480–485.
23. Muckenfuss,H., Hamdorf,M., Held,U., Perkovic,M., Lower,J., Cichutek,K., Flory,E., Schumann,G.G. and Munk,C. (2006)

APOBEC3 proteins inhibit human LINE-1 retrotransposition. *J. Biol. Chem.*, **281**, 22161–22172.
24. Stenglein,M.D. and Harris,R.S. (2006) APOBEC3B and APOBEC3F inhibit L1 retrotransposition by a DNA deamination-independent mechanism. *J. Biol. Chem.*, **281**, 16837–16841.
25. Fisher,A.G., Ensoli,B., Ivanoff,L., Chamberlain,M., Petteway,S., Ratner,L., Gallo,R.C. and Wong-Staal,F. (1987) The *sor* gene of HIV-1 is required for efficient virus transmission in vitro. *Science*, **237**, 888–893.
26. Strebel,K., Daugherty,D., Clouse,K., Cohen,D., Folks,T. and Martin,M.A. (1987) The HIV 'A' (sor) gene product is essential for virus infectivity. *Nature*, **328**, 728–730.
27. Fouchier,R.A., Simon,J.H., Jaffe,A.B. and Malim,M.H. (1996) Human immunodeficiency virus type 1 Vif does not influence expression or virion incorporation of *gag*-, *pol*-, and *env*-encoded proteins. *J. Virol.*, **70**, 8263–8269.
28. Sova,P. and Volsky,D.J. (1993) Efficiency of viral DNA synthesis during infection of permissive and nonpermissive cells with *vif*-negative human immunodeficiency virus type 1. *J. Virol.*, **67**, 6322–6326.
29. von Schwedler,U., Song,J., Aiken,C. and Trono,D. (1993) *vif* is crucial for human immunodeficiency virus type 1 proviral DNA synthesis in infected cells. *J. Virol.*, **67**, 4945–4955.
30. Goncalves,J., Korin,Y., Zack,J. and Gabuzda,D. (1996) Role of Vif in human immunodeficiency virus type 1 reverse transcription. *J. Virol.*, **70**, 8701–8709.
31. Simon,J.H. and Malim,M.H. (1996) The human immunodeficiency virus type 1 Vif protein modulates the postpenetration stability of viral nucleoprotein complexes. *J. Virol.*, **70**, 5297–5305.
32. Dettenhofer,M., Cen,S., Carlson,B.A., Kleiman,L. and Yu,X.F. (2000) Association of human immunodeficiency virus type 1 Vif with RNA and its role in reverse transcription. *J. Virol.*, **74**, 8938–8945.
33. Dornadula,G., Yang,S., Pomerantz,R.J. and Zhang,H. (2000) Partial rescue of the Vif-negative phenotype of mutant human immunodeficiency virus type 1 strains from nonpermissive cells by intravirion reverse transcription. *J. Virol.*, **74**, 2594–2602.
34. Li,J., Potash,M.J. and Volsky,D.J. (2004) Functional domains of APOBEC3G required for antiviral activity. *J. Cell. Biochem.*, **92**, 560–572.
35. Guo,F., Cen,S., Niu,M., Saadatmand,J. and Kleiman,L. (2006) Inhibition of $tRNA_3^{Lys}$-primed reverse transcription by human APOBEC3G during human immunodeficiency virus type 1 replication. *J. Virol.*, **80**, 11710–11722.
36. Kaiser,S.M. and Emerman,M. (2006) Uracil DNA glycosylase is dispensable for human immunodeficiency virus type 1 replication and does not contribute to the antiviral effects of the cytidine deaminase Apobec3G. *J. Virol.*, **80**, 875–882.
37. Mbisa,J.L., Barr,R., Thomas,J.A., Vandegraaff,N., Dorweiler,I.J., Svarovskaia,E.S., Brown,W.L., Mansky,L.M., Gorelick,R.J. *et al.* (2007) Human immunodeficiency virus type 1 cDNAs produced in the presence of APOBEC3G exhibit defects in plus-strand DNA transfer and integration. *J. Virol.*, **81**, 7099–7110.
38. Yang,Y., Guo,F., Cen,S. and Kleiman,L. (2007) Inhibition of initiation of reverse transcription in HIV-1 by human APOBEC3F. *Virology*, **365**, 92–100.
39. Herschlag,D. (1995) RNA chaperones and the RNA folding problem. *J. Biol. Chem.*, **270**, 20871–20874.
40. Darlix,J.L., Lapadat-Tapolsky,M., de Rocquigny,H. and Roques,B.P. (1995) First glimpses at structure-function relationships of the nucleocapsid protein of retroviruses. *J. Mol. Biol.*, **254**, 523–537.
41. Rein,A., Henderson,L.E. and Levin,J.G. (1998) Nucleic-acid-chaperone activity of retroviral nucleocapsid proteins: significance for viral replication. *Trends Biochem. Sci.*, **23**, 297–301.
42. Cristofari,G. and Darlix,J.L. (2002) The ubiquitous nature of RNA chaperone proteins. *Prog. Nucleic Acid Res. Mol. Biol.*, **72**, 223–268.
43. Levin,J.G., Guo,J., Rouzina,I. and Musier-Forsyth,K. (2005) Nucleic acid chaperone activity of HIV-1 nucleocapsid protein: critical role in reverse transcription and molecular mechanism. *Prog. Nucleic Acid Res. Mol. Biol.*, **80**, 217–286.
44. Tsuchihashi,Z. and Brown,P.O. (1994) DNA strand exchange and selective DNA annealing promoted by the human immunodeficiency virus type 1 nucleocapsid protein. *J. Virol.*, **68**, 5863–5870.
45. Jarmuz,A., Chester,A., Bayliss,J., Gisbourne,J., Dunham,I., Scott,J. and Navaratnam,N. (2002) An anthropoid-specific locus of orphan C to U RNA-editing enzymes on chromosome 22. *Genomics*, **79**, 285–296.
46. Cruceanu,M., Urbaneja,M.A., Hixson,C.V., Johnson,D.G., Datta,S.A., Fivash,M.J., Stephen,A.G., Fisher,R.J., Gorelick,R.J. *et al.* (2006) Nucleic acid binding and chaperone properties of HIV-1 Gag and nucleocapsid proteins. *Nucleic Acids Res.*, **34**, 593–605.
47. Fisher,R.J., Fivash,M.J., Stephen,A.G., Hagan,N.A., Shenoy,S.R., Medaglia,M.V., Smith,L.R., Worthy,K.M., Simpson,J.T. *et al.* (2006) Complex interactions of HIV-1 nucleocapsid protein with oligonucleotides. *Nucleic Acids Res.*, **34**, 472–484.
48. Powell,M.D. and Levin,J.G. (1996) Sequence and structural determinants required for priming of plus-strand DNA synthesis by the human immunodeficiency virus type 1 polypurine tract. *J. Virol.*, **70**, 5288–5296.
49. Guo,J., Henderson,L.E., Bess,J., Kane,B. and Levin,J.G. (1997) Human immunodeficiency virus type 1 nucleocapsid protein promotes efficient strand transfer and specific viral DNA synthesis by inhibiting TAR-dependent self-priming from minus-strand strong-stop DNA. *J. Virol.*, **71**, 5178–5188.
50. Wu,T., Guo,J., Bess,J., Henderson,L.E. and Levin,J.G. (1999) Molecular requirements for human immunodeficiency virus type 1 plus-strand transfer: analysis in reconstituted and endogenous reverse transcription systems. *J. Virol.*, **73**, 4794–4805.
51. Iwatani,Y., Rosen,A.E., Guo,J., Musier-Forsyth,K. and Levin,J.G. (2003) Efficient initiation of HIV-1 reverse transcription in vitro. Requirement for RNA sequences downstream of the primer binding site abrogated by nucleocapsid protein-dependent primer-template interactions. *J. Biol. Chem.*, **278**, 14185–14195.
52. Wu,W., Henderson,L.E., Copeland,T.D., Gorelick,R.J., Bosche,W.J., Rein,A. and Levin,J.G. (1996) Human immunodeficiency virus type 1 nucleocapsid protein reduces reverse transcriptase pausing at a secondary structure near the murine leukemia virus polypurine tract. *J. Virol.*, **70**, 7132–7142.
53. Lee,N., Gorelick,R.J. and Musier-Forsyth,K. (2003) Zinc finger-dependent HIV-1 nucleocapsid protein-TAR RNA interactions. *Nucleic Acids Res.*, **31**, 4847–4855.
54. Adachi,A., Gendelman,H.E., Koenig,S., Folks,T., Willey,R., Rabson,A. and Martin,M.A. (1986) Production of acquired immunodeficiency syndrome-associated retrovirus in human and nonhuman cells transfected with an infectious molecular clone. *J. Virol.*, **59**, 284–291.
55. Guo,J., Wu,W., Yuan,Z.Y., Post,K., Crouch,R.J. and Levin,J.G. (1995) Defects in primer-template binding, processive DNA synthesis, and RNase H activity associated with chimeric reverse transcriptases having the murine leukemia virus polymerase domain joined to *Escherichia coli* RNase H. *Biochemistry*, **34**, 5018–5029.
56. Guo,J., Wu,T., Bess,J., Henderson,L.E. and Levin,J.G. (1998) Actinomycin D inhibits human immunodeficiency virus type 1 minus-strand transfer in in vitro and endogenous reverse transcriptase assays. *J. Virol.*, **72**, 6716–6724.
57. Powell,M.D., Ghosh,M., Jacques,P.S., Howard,K.J., Le Grice,S.F. and Levin,J.G. (1997) Alanine-scanning mutations in the "primer grip" of p66 HIV-1 reverse transcriptase result in selective loss of RNA priming activity. *J. Biol. Chem.*, **272**, 13262–13269.
58. McCauley,M., Hardwidge,P.R., Maher,L.J.III and Williams,M.C. (2005) Dual binding modes for an HMG domain from human HMGB2 on DNA. *Biophys. J.*, **89**, 353–364.
59. McCauley,M.J. and Williams,M.C. (2007) Mechanisms of DNA binding determined in optical tweezers experiments. *Biopolymers*, **85**, 154–168.
60. Cruceanu,M., Gorelick,R.J., Musier-Forsyth,K., Rouzina,I. and Williams,M.C. (2006) Rapid kinetics of protein-nucleic acid interaction is a major component of HIV-1 nucleocapsid protein's nucleic acid chaperone function. *J. Mol. Biol.*, **363**, 867–877.

61. Lundblad,J.R., Laurance,M. and Goodman,R.H. (1996) Fluorescence polarization analysis of protein-DNA and protein-protein interactions. *Mol. Endocrinol.*, **10**, 607–612.
62. Lakowicz,J.R. (1999) *Principles of Fluorescence Spectroscopy*. Kluwer Academic/Plenum, New York.
63. Guo,J., Wu,T., Anderson,J., Kane,B.F., Johnson,D.G., Gorelick,R.J., Henderson,L.E. and Levin,J.G. (2000) Zinc finger structures in the human immunodeficiency virus type 1 nucleocapsid protein facilitate efficient minus- and plus-strand transfer. *J. Virol.*, **74**, 8980–8988.
64. Hong,M.K., Harbron,E.J., O'Connor,D.B., Guo,J., Barbara,P.F., Levin,J.G. and Musier-Forsyth,K. (2003) Nucleic acid conformational changes essential for HIV-1 nucleocapsid protein-mediated inhibition of self-priming in minus-strand transfer. *J. Mol. Biol.*, **325**, 1–10.
65. Heilman-Miller,S.L., Wu,T. and Levin,J.G. (2004) Alteration of nucleic acid structure and stability modulates the efficiency of minus-strand transfer mediated by the HIV-1 nucleocapsid protein. *J. Biol. Chem.*, **279**, 44154–44165.
66. Chelico,L., Pham,P., Calabrese,P. and Goodman,M.F. (2006) APOBEC3G DNA deaminase acts processively 3′ -> 5′ on single-stranded DNA. *Nat. Struct. Mol. Biol.*, **13**, 392–399.
67. Guo,F., Cen,S., Niu,M., Yang,Y., Gorelick,R.J. and Kleiman,L. (2007) The interaction of APOBEC3G with HIV-1 nucleocapsid inhibits $tRNA_3^{Lys}$ annealing to viral RNA, *J. Virol.*, **81**, 11322–11331
68. Xu,H., Chertova,E., Chen,J., Ott,D.E., Roser,J.D., Hu,W.S. and Pathak,V.K. (2007) Stoichiometry of the antiviral protein APOBEC3G in HIV-1 virions. *Virology*, **360**, 247–256.
69. Briggs,J.A., Wilk,T., Welker,R., Kräusslich,H.G. and Fuller,S.D. (2003) Structural organization of authentic, mature HIV-1 virions and cores. *EMBO J.*, **22**, 1707–1715.
70. Darlix,J.L., Schwager,M., Spahr,P.F. and Bromley,P.A. (1980) Analysis of the secondary and tertiary structures of Rous sarcoma virus RNA. *Nucleic Acids Res.*, **8**, 3335–3354.
71. Murti,K.G., Bondurant,M. and Tereba,A. (1981) Secondary structural features in the 70S RNAs of Moloney murine leukemia and Rous sarcoma viruses as observed by electron microscopy. *J. Virol.*, **37**, 411–419.
72. Berkhout,B. and van Wamel,J.L. (2000) The leader of the HIV-1 RNA genome forms a compactly folded tertiary structure. *RNA*, **6**, 282–295.
73. Shokri,L., Marintcheva,B., Richardson,C.C., Rouzina,I. and Williams,M.C. (2006) Single molecule force spectroscopy of salt-dependent bacteriophage T7 gene 2.5 protein binding to single-stranded DNA. *J. Biol. Chem.*, **281**, 38689–38696.

JOURNAL OF CLINICAL MICROBIOLOGY, Feb. 2007, p. 477–487 Vol. 45, No. 2
0095-1137/07/$08.00+0 doi:10.1128/JCM.01708-06

Use of New T-Cell-Based Cell Lines Expressing Two Luciferase Reporters for Accurately Evaluating Susceptibility to Anti-Human Immunodeficiency Virus Type 1 Drugs[▽]

Tomoko Chiba-Mizutani,[1,2] Hideka Miura,[1] Masakazu Matsuda,[1] Zene Matsuda,[1] Yoshiyuki Yokomaku,[1] Kosuke Miyauchi,[1] Masako Nishizawa,[1] Naoki Yamamoto,[1,2] and Wataru Sugiura[1]*

AIDS Research Center, National Institute of Infectious Diseases, Tokyo, Japan,[1] and Department of Molecular Virology and Microbiology, Tokyo Medical and Dental University, Tokyo, Japan[2]

Received 17 August 2006/Returned for modification 25 October 2006/Accepted 11 December 2006

Two new T-cell-based reporter cell lines were established to measure human immunodeficiency virus type 1 (HIV-1) infectivity. One cell line naturally expresses CD4 and CXCR4, making it susceptible to X4-tropic viruses, and the other cell line, in which a CCR5 expression vector was introduced, is susceptible to both X4- and R5-tropic viruses. Reporter cells were constructed by transfecting the human T-cell line HPB-Ma, which demonstrates high susceptibility to HIV-1, with genomes expressing two different luciferase reporters, HIV-1 long terminal repeat-driven firefly luciferase and cytomegalovirus promoter-driven renilla luciferase. Upon HIV infection, the cells expressed firefly luciferase at levels that were highly correlated (r^2 = 0.91 to 0.98) with the production of the capsid antigen p24. The cells also constitutively expressed renilla luciferase, which was used to monitor cell numbers and viability. The reliability of the cell lines for two in vitro applications, drug resistance phenotyping and drug screening, was confirmed. As HIV-1 efficiently replicated in these cells, they could be used for multiple-round replication assays as an alternative method to a single-cycle replication protocol. Coefficients of variation for drug susceptibility evaluated with the cell lines ranged from 17 to 41%. The new cell lines were beneficial for evaluating antiretroviral drug resistance. Firefly luciferase gave a wider dynamic range for evaluating virus infectivity, and the introduction of renilla luciferase improved assay reproducibility. The cell lines were also beneficial for screening new antiretroviral agents, as false inhibition caused by the cytotoxicity of test compounds was easily detected by monitoring renilla luciferase activity.

Drug resistance assays have been accepted as standard clinical tests to guide the antiretroviral therapy of human immunodeficiency virus (HIV)-infected patients who have developed resistance to drug treatment or drug-naïve patients infected with drug-resistant virus. These tests have been shown to improve treatment outcomes by selecting the most effective drugs and by minimizing the risk of treatment failure (2, 5–7, 9, 34). Drug resistance has been determined by two approaches. One is drug resistance genotyping, in which drug resistance is evaluated by sequencing the viral genes targeted by the drug, such as the HIV-1 protease and reverse transcriptase (RT) genes. The level of drug resistance is estimated by using observed mutation patterns and interpretation algorithms (23). Several protocols have been used for drug resistance genotyping, including in-house sequencing (10, 13, 38). Although these protocols differ in some aspects, e.g., the design of primers, the length of analyses, and amplification procedures, all are based on the same technical approach, modified Sanger sequencing.

The other approach to drug resistance assays is phenotyping. In this method, the levels of drug resistance of patient-derived viral isolates are evaluated by using in vitro bioassays (17, 26). Two advantages of the phenotyping assay are its ability to directly evaluate the drug susceptibilities of patient-derived viruses and the ease of interpreting its results compared to those from genotyping. This assay is especially useful in cases with a high degree of exposure to antiretroviral drugs, therefore involving many mutations. In these cases, the evaluation of resistance levels by genotyping alone may be difficult (35). In addition, the resistance levels determined by phenotyping provide important information for updating interpretation algorithms used in genotyping.

Although peripheral blood mononuclear cells (PBMC) are the natural target of HIV type 1 (HIV-1) and hence are the best candidates for host cells in phenotyping assays, reporter cell systems are more commonly used in drug susceptibility assays (1, 12, 15, 31). Reporter systems are preferred because their susceptibility to HIV-1 is stable and their output is both rapidly measured and highly reproducible compared to that of PBMC assays. Several kinds of reporter cells have been used with different reporter proteins, such as MAGI cells with β-galactosidase (21), GHOST cells with enhanced green fluorescent protein (36), MOCHA cells with secreted alkaline phosphatase (24), and CEM.NKR-CCR5-Luc cells with luciferase (31). Although these systems use different cell lines, their basic strategies for evaluating HIV infectivity are similar (21, 36). The cell lines carry a reporter protein gene regulated by the HIV-1 long terminal repeat (LTR) promoter, inducing them to

* Corresponding author. Mailing address: AIDS Research Center, National Institute of Infectious Diseases, 4-7-1 Gakuenn, Musashimurayama, Tokyo 2080011, Japan. Phone: 81-42-561-0771. Fax: 81-42-561-7746. E-mail: wsugiura@nih.go.jp.

▽ Published ahead of print on 20 December 2006.

produce the reporter protein when they are infected with HIV-1. Which reporter system is used depends on the properties of the original cell line and the installed reporter protein.

Reporter systems using MAGI and GHOST cells have the advantages of high sensitivity and rapidity in determining infectivity. However, MAGI and GHOST cells have been established from HeLa cells (21) and human osteosarcoma cells (36), respectively, which are not naturally susceptible to HIV-1. Therefore, these cells cannot propagate viruses efficiently. On the other hand, MOCHA and CEM.NKR-CCR5-Luc cell lines were established from T-cell lines and secreted alkaline phosphatase and luciferase, respectively, were installed as reporters. These reporter systems allow for the evaluation of HIV-1 infectivity by using enzymatic reactions and demonstrate greater reproducibility with wider dynamic ranges of reporter proteins. However, for these cells to produce sufficient reporter protein for accurate determinations, they must be cultured for 5 to 7 days, longer than MAGI and GHOST cells. Longer culture periods allow reporter cells to divide, which may affect the accuracy of the quantification.

Given the advantages and limitations of previously constructed reporter cell lines, we designed and tested two new reporter cell lines with dual chemokine receptors for use in drug resistance phenotypic assays and other HIV infectivity assays. The cell lines we designed have unique characteristics in that they originate from the human T-cell line HPB-Ma (16, 29, 40) and were engineered to express the CCR5 receptor and two different marker proteins, firefly luciferase (FL) and renilla luciferase (RL). FL, which is under HIV-1 LTR promoter regulation, is produced upon HIV-1 infection. Therefore, firefly luciferase activity can be used as a marker for virus infectivity. RL, which is under cytomegalovirus (CMV) promoter control, is constitutively expressed in the cells. Therefore, renilla luciferase activity can be used as a marker for cell number and viability.

MATERIALS AND METHODS

Construction of luciferase and CCR5 expression vectors. Two different luciferase expression vectors were constructed. The first luciferase construct comprised HIV-1 Tat-regulated FL and the red fluorescent protein (DsRed) construct 53LTRN-lucneo^r#1. The HIV-1 Tat-responsive reporter construct 53LTRN-lucneo^r#1 was constructed based on the expression vector pGEM-7Zf(+) (Promega, Madison, WI). Initially, a parent vector was constructed, 53LTRNCNS, which has a rabbit β-globin unit under the control of the HIV-1 LTR derived from strain HXB2. In this construct, a gene of interest can be cloned within the second exon of the β-globin gene and the polyadenylation signal is provided by the β-globin unit. A neomycin expression module was prepared by PCR and cloned upstream of the HIV-1 LTR region to generate 53LTRCNSneo. The reporter gene employed here was a fusion between an FL gene and a DsRed gene. The FL gene allows HIV-1 replication to be quantitatively evaluated by using luciferase activity when the LTR is activated by HIV-derived Tat, and the DsRed gene allows transfected and HIV-infected cells to be identified by red fluorescence. The FL portion was derived from pGLuc5 (Promega), and the DsRed portion was derived from pDsRed1N-1 (Clontech). Both genes were prepared by PCR, fused, and cloned into the β-globin unit by using NcoI and NotI restriction sites.

The second luciferase construct, pRenillaPac, was constructed using the plasmid pPUR (Clontech). The PCR-amplified RL gene, derived from phRL-CMV (Promega), was spliced into the upstream region of the *pac* gene. This hybrid gene manifests both RL activity and resistance to puromycin. Expression of the fusion gene was constitutive under the control of a CMV promoter.

A CCR5 expression vector, pCCR5/CEP4, was constructed based on the pCEP4 expression vector (Invitrogen), which possesses the Epstein-Barr nuclear antigen 1 episomal-expression gene. The CCR5 gene was inserted into the vector by using NotI and SnaB I restriction sites on the vector. Expression of the CCR5 gene was constitutive under the control of a CMV promoter.

Selection of host cell line and establishment of new reporter cell lines. To design new reporter cell lines for quantifying HIV-1 replication, we selected the murine leukemia virus-transformed human T-cell line HPB-Ma, established by Y. K. Shimizu and H. Yoshikura (16, 29, 40), because of its high susceptibility to HIV-1 and its stable expression of CD4 and CXCR4. HPB-Ma cells were maintained at 37°C in 5% CO_2 in complete RPMI 1640 medium (Sigma, Tokyo, Japan) supplemented with 10% fetal calf serum (HyClone, Logan, UT) and 1% penicillin-streptomycin (Invitrogen, Tokyo, Japan). Cells were transfected by electroporation with the two luciferase expression vectors, 53LTRN-lucneo^r#1 and pRenillaPac. Plasmid DNA (10 μg) was mixed with HPB-Ma cells (5×10^6 cells in 500 μl phosphate-buffered saline), and the mixture was incubated for 5 min at 4°C and electropulsed with a Gene Pulser II apparatus (Bio-Rad, Hercules, CA) at 250 V and 950 μF. After electroporation, the cells were resuspended in complete medium and incubated at 37°C in 5% CO_2. Subsequently, cells with incorporated plasmids were selected with 0.1 μg/ml puromycin (BD Biosciences, San Jose, CA) and 250 μg/ml Geneticin (Invitrogen), maintained in complete medium for several weeks, and enriched with cell populations expressing high levels of CD4 and CXCR4 by fluorescence-activated cell sorting with a FACSVantage system (BD Biosciences). Finally, clones were generated by limiting dilution and selected if they showed high sensitivity to HIV-1 and low spontaneous expression of FL and DsRed.

Since the parent HPB-Ma cell line expresses only the CXCR4 receptor, we extended the spectrum of the reporter cell lines to include R5-tropic viral isolates by transfecting cells by electroporation with a CCR5 expression plasmid. Clones were selected by incubating for several weeks with 0.1 μg/ml puromycin, 250 μg/ml Geneticin, and 150 μg/ml hygromycin B. Selected cells were recloned, and the expression of cell surface markers was confirmed by using FACSCaliber (Becton Dickinson, San Jose, CA). CD4, CXCR4, and CCR5 receptors were stained with SK-3-Cy5.5, 12G5-phycoerythrin, and 2D7-fluorescein isothiocyanate monoclonal antibodies, respectively (all from BD Biosciences, San Jose, CA).

Evaluation of introduced reporter gene functions. To confirm the ability of FL activity to reliably measure virus titer and production, established cell lines were plated into 96-well plates at 10^5 cells per well and inoculated with 50 to 400 50% tissue culture infective doses ($TCID_{50}$) of HXB2 or JRCSF. After 7 days of culture with the test viruses, cells were harvested and lysed in 75 μl of luciferase assay reagent. FL activity was quantified using a Dual-Glo luciferase reporter assay system (Promega, Madison, WI) and an LMax microplate luminometer (Molecular Devices, Sunnyvale, CA). Virus production was also quantified by using the p24 antigen enzyme-linked immunosorbent assay RETROtek kit (ZeproMetrix Co., Buffalo, NY) and compared with FL activity.

The validity of using RL activity to monitor MaRBLE cell numbers was evaluated by measuring RL activity in various numbers of cells and determining the correlation between RL activity and cell numbers. The correlation between RL activity and cell viability was also confirmed in cell killing assays with two anticancer drugs, hygromycin B (Invitrogen, Tokyo, Japan) and blasticidin S (Funakoshi, Tokyo, Japan). Target cells were plated into 96-well plates at 10^5 cells per well, and hygromycin B (15.6 to 500 μg/ml) and blasticidin S (1.25 to 20 μg/ml) were added. After 7 days of culture, cells were harvested and RL activity was measured by using the Dual-Glo luciferase reporter assay system (Promega) and the percentage of cell killing was determined by trypan blue staining.

Preparation of recombinant and patient-derived viruses. Recombinant viruses with point mutations were constructed as described elsewhere (25). In brief, drug resistance mutations were introduced into the RT and protease genes of the HXB2 clone by site-directed mutagenesis (28). MT-2 cells (5×10^6 human T-lymphoblastoid cells) were then transfected by electroporation with the recombinant virus plasmids, and the cells were maintained in 10 ml of complete medium for 7 to 14 days. Half the culture supernatant was harvested and replaced with fresh medium every other day. Viral replication was monitored by measuring RT activity in the supernatant, and the sample with the highest RT activity was used in subsequent studies.

Eight clinical samples were selected randomly from patient blood specimens sent for routine HIV-1 drug resistance testing to the AIDS Research Center, National Institute of Infectious Diseases, Tokyo, Japan. Patient viruses were isolated by a standard coculture method described elsewhere (18). In brief, 2×10^7 patient PBMC were mixed with the same number of phytohemagglutinin-stimulated normal human PBMC and the mixture was cultured for 2 weeks. Half the culture supernatant was collected and replaced with the same amount of fresh culture medium every other day. Viral replication was monitored by mea-

suring RT activity in the supernatant, and the sample with peak RT activity was selected and used for infection experiments afterward. RT assays were performed as previously described (37). Viral RNAs in collected supernatants were sequenced, and drug resistance mutation patterns were determined.

For the reconstructed virus, viral RNA was extracted from 200 μl of patient plasma by using a High Pure viral RNA kit (Roche, Basel, Switzerland) according to the manufacturer's instructions. Subsequently, a 1.8-kb *gag-pol* fragment, encoding the region from $p2^{gag}$ to whole protease, and the 5′ half of the RT gene fragment were amplified and inserted into the HXB2 backbone. MT-2 cells (5×10^6) were then transfected by electroporation with the plasmid, and the cells were maintained in 10 ml of complete medium for 7 to 14 days. Half the culture supernatant was harvested and replaced with fresh medium every other day. Viral replication was monitored by measuring RT activity in the supernatant, and the sample with the highest RT activity was selected for use in subsequent studies. Viral RNAs in collected supernatants were sequenced, and the drug resistance mutation patterns were confirmed. For both the patient-derived and reconstructed viruses, HIV infectivity ($TCID_{50}$) in the target cell lines was assayed by the Reed-Muench method (27).

Drug resistance genotyping. HIV-1 RNA was extracted from 200 μl of patient plasma using a High Pure viral RNA kit according to the manufacturer's instructions. For amplification of the 500-bp protease gene fragment, DRPRO5 (5′-AGA-CAG-GYT-AAT-TTT-TTA-GGG-A) and DRPRO2L (5′-TAT-GGA-TTT-TCA-GGC-CCA-ATT-TTT-GA) were used for reverse transcription and the first PCR and DRPRO1M (5′-AGA-GCC-AAC-AGC-CCC-ACC-AG) and DRPRO6 (5′-ACT-TTT-GGG-CCA-TCC-ATT-CC) were used for the second PCR. For amplification of the 800-bp RT gene fragment, DRRT1L (5′-ATG-ATA-GGG-GGA-ATT-GGA-GGT-TT) and DRRT4L (5′-TAC-TTC-TGT-TAG-TGC-TTT-GGT-TCC) were used for reverse transcription and the first PCR and DRRT7L (5′-GAC-CTA-CAC-CTG-TCA-ACA-TAA-TTG-G) and DRRT6L (5′-TAA-TCC-CTG-CAT-AAA-TCT-GAC-TTG-C) were used for the second PCR. The amplicons were purified by using a MultiScreen PCR filter plate (Millipore), and sequence reactions were performed by using the BigDye Terminator v3.1 cycle sequencing kit, followed by electrophoresis using an ABI-3730 auto sequencer (Applied Biosystems, Foster City, CA).

HIV-1 replication kinetics analyses and drug susceptibility assays. To analyze the replication kinetics of clinically derived HIV-1 isolates, target cells were plated into 96-well plates at 10^5 cells per well and infected with 100 $TCID_{50}$ of test viruses per well. At days 3, 5, and 7, the culture supernatant of each well was collected and RT activity was measured as previously described (37).

To evaluate anti-HIV-1 drug susceptibility, 10^7 cells were infected with 10,000 $TCID_{50}$ of wild-type control or test viruses in 50-ml tubes and incubated for 2 h at 37°C. Infected cells were resuspended in culture medium and plated into 96-well plates at 10^5 cells per well. At 2 and 48 h after infection, serial RT inhibitor dilutions and serial protease inhibitor (PI) dilutions were added, respectively. Each drug was prepared in a fivefold serial dilution and tested over different dose ranges, as follows. Didanosine, abacavir, and nevirapine were tested at concentrations from 25.0×10^1 μm to 3.2×10^{-4} μM. Lamivudine and stavudine were tested at concentrations from 5.0×10^1 μm to 6.4×10^{-5} μM. Zidovudine, zalcitabine, and the five PIs (saquinavir, indinavir, nelfinavir, lopinavir, and amprenavir) were tested at concentrations from 1.0×10^1 μm to 12.8×10^{-6} μM. Efavirenz was tested at concentrations from 0.2×10^1 μm to 25.6×10^{-7} μM. All samples were tested in triplicate. The following manufacturers kindly supplied anti-HIV drugs: GlaxoSmithKline, Middlesex, United Kingdom (zidovudine, lamivudine, and abacavir); Bristol-Myers Squibb, New York, NY (didanosine, stavudine, and efavirenz); Roche, Basel, Switzerland (zalcitabine and saquinavir); Boehringer Ingelheim, Ingelheim, Germany (nevirapine); Merck Research Laboratories, Rahway, NJ (indinavir); Japan Tobacco, Tokyo, Japan (nelfinavir); Vertex Pharmaceuticals, Cambridge, MA (amprenavir); and Abbott Laboratories, Abbott Park, IL (lopinavir).

After 7 days of culture with test drugs and test viruses, cells were harvested and lysed in 75 μl of luciferase assay reagent. Firefly and RL activities were sequentially quantified using a dual-luciferase reporter assay system (Promega) and an LMax microplate luminometer (Molecular Devices). Data were displayed by plotting the percentage of luciferase activity versus the $\log_{10}$ drug concentration. The concentration at which 50% of viral replication was inhibited (IC_{50}) was determined by plotting curves defined by the four-parametric sigmoidal equation $f(x) = A + ([B - A])/(1 + [C/x]^D)$ using XLfit4 software (CTC Laboratory Systems Corporation, Tokyo, Japan). To determine susceptibility or resistance, results for test viruses were compared to those for wild-type HIV-1 and evaluated by Student's *t* test.

RESULTS

Establishment of new T-cell-based cell lines with two luciferase reporter proteins. Two luciferase expression vectors were successfully constructed and used for transfection of the HPB-Ma cell line. These vectors were 53LTRN-lucneo^r#1, with FL under HIV-1 LTR regulation, and pRenillaPac, with RL under CMV promoter regulation. HPB-Ma cells with these vectors were subjected to several rounds of selection for cells resistant to Geneticin and puromycin and were enriched by flow cytometry with populations expressing high levels of CD4 and CXCR4 to establish the new cell line HPB-Ma/LTR-FL/CMV-RL (X4-MaRBLE).

Since the parent HPB-Ma cell line expresses only CXCR4, the spectrum of the X4-MaRBLE cell line was extended to include R5-tropic viruses by transfection with a CCR5 expression plasmid, thus establishing the R5-MaRBLE cell line. Expression levels of CD4 were comparable among the parent HPB-Ma, X4-MaRBLE, and R5-MaRBLE cell lines (Fig. 1a to c), whereas the proportion of CXCR4-positive cell populations and CXCR4 expression levels were slightly higher in X4- and R5-MaRBLE cells than in the parent HPB-Ma cell line (Fig. 1d to f). This difference is due to the cell sorter's selecting for populations expressing high levels of CXCR4. As for CCR5 expression, HPB-Ma and X4-MaRBLE cells did not significantly express the receptor (Fig. 1g and h). On the other hand, more than 76% of the R5-MaRBLE cell population expressed CCR5 (Fig. 1i).

To confirm the susceptibility of cell lines to X4- and R5-tropic viruses, each cell line was inoculated with HXB2 (X4-tropic) and JRCSF (R5-tropic) viruses. X4-MaRBLE cells inoculated with HXB2 expressed FL activity in a dose-dependent manner but did not show any FL activity after inoculation with JRCSF (Fig. 2a). On the other hand, R5-MaRBLE cells were susceptible to both HXB2 and JRCSF, which induced FL activity in a dose-dependent manner (Fig. 2b). To validate the use of FL activity to evaluate viral production, FL levels were compared to amounts of the viral capsid antigen, p24, in both X4- and R5-MaRBLE cell lines, and the correlation between FL levels and the amounts of p24 was determined. As shown in Fig. 2c, FL activity in cell lysates and the amount of p24 antigen in the culture supernatant were positively and linearly correlated in X4-MaRBLE cells infected with HXB2 ($r^2 = 0.98$), in R5-MaRBLE cells infected with HXB2 ($r^2 = 0.91$), and in R5-MaRBLE cells infected with JRCSF ($r^2 = 0.94$). These results verify that FL activity expressed by both X4- and R5-MaRBLE cell lines accurately represents the levels of viral replication and production. These good correlations also indicate a small likelihood of interference between the two LTRs in infected cells, the one driving luciferase and the other contained in the infecting virus.

The second type of luciferase, RL, was inserted into MaRBLE cells to monitor and evaluate their number and viability. As shown in Fig. 3a, RL activity demonstrated a positive, linear correlation with cell number ($r^2 = 0.99$). Thus, RL activity can be used to assess cell number in culture. Another useful parameter evaluated by RL activity was the cytotoxicity of test compounds added to cultures. To confirm the relationship between RL activity and cell viability, cell killing assays were performed with two anticancer drugs, hygromycin

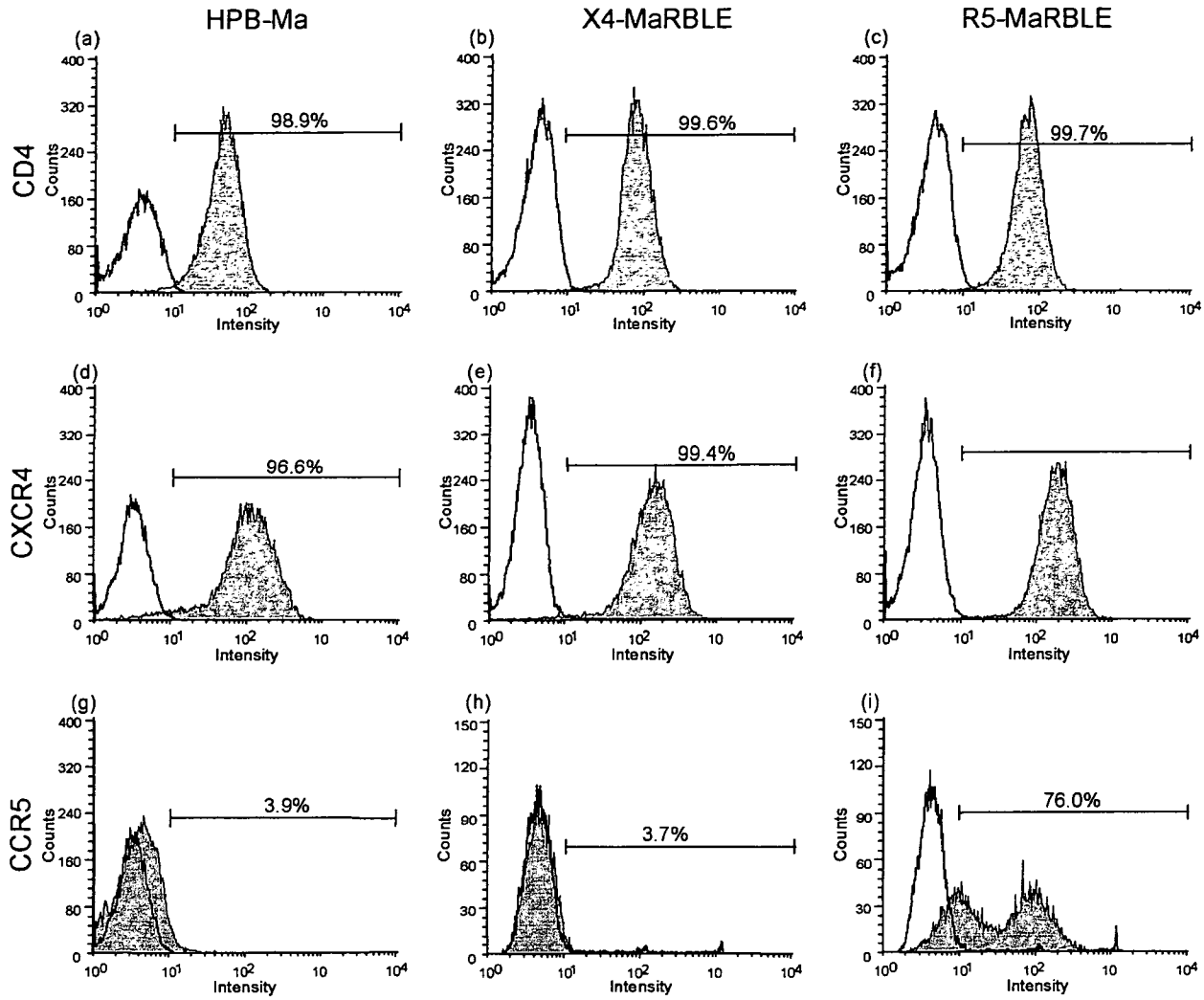

FIG. 1. Levels of expression of CD4, CXCR4, and CCR5 in parent HPB-Ma cells and X4-MaRBLE and R5-MaRBLE cells. Parent HPB-Ma (a, d, g), X4-MaRBLE (b, e, h), and R5-MaRBLE (c, f, i) cells were stained with monoclonal antibodies to CD4 (a, b, c), CXCR4 (d, e, f), and CCR5 (g, h, i). To calculate the percentage of each population positive for the expression of cytokine receptors (bars), 2,000 to 5,000 cells were analyzed by fluorescence-activated cell sorting. To calculate the percentage of each population positive for expression of CD4 and cytokine receptors (bar), 2,000 to 5,000 cells were analyzed by FACSCalibur and compared with fluorescence-negative control cells. Histograms with gray shading indicate cell populations stained with each monoclonal antibody; histograms without shading indicate negative control populations.

B (Fig. 3b) and blasticidin S (Fig. 3c). As the percentages of cells killed by both test chemicals increased, RL activity declined (Fig. 3b and c). The concentrations of hygromycin B and blasticidin S needed to kill 50% of the cells were 100 μg/ml and 2 μg/ml, respectively, in agreement with data from previous reports (3, 32). Thus, RL activity can be used to measure cytotoxicity.

In addition, the replication of two patient-derived viral isolates, 8 and 9, in R5-MaRBLE cells was compared to that in PBMC. As shown in Fig. 4, the two clinical isolates efficiently replicated in R5-MaRBLE cells. Isolate 8 replicated more efficiently in R5-MaRBLE cells than in PBMC, as indicated by the 10-fold-higher RT activity at day 7 in R5-MaRBLE cells (Fig. 4a). Isolate 9 had comparable day 7 RT activities in R5-MaRBLE cells and PBMC (Fig. 4b). These data clearly show that R5-MaRBLE cells can efficiently propagate clinical isolates.

Evaluation of HIV-1 drug susceptibility using X4- and R5-MaRBLE cells is highly reproducible. Having confirmed the quantitative reliability of FL expressed by HIV-infected X4- and R5-MaRBLE cell lines, we next used the cell lines to evaluate HIV-1 susceptibility to antiretroviral drugs. First, we evaluated the precision of phenotyping using the X4- and R5-MaRBLE cell lines. By using the wild-type HXB2 strain as a target virus for both X4- and R5-MaRBLE cells and JRCSF as a target virus for R5-MaRBLE cells, the IC_{50}s of four representative drugs from three classes of antiretroviral agents (zidovudine, lamivudine, efavirenz, and lopinavir) were determined by measuring FL activity. As shown in Fig. 5, well-characterized dose-response curves were obtained for the four drugs. The mean IC_{50}s, standard deviations (SD), and coefficients of variation (CV) for each cell line are summarized in Table 1. The CV ranged from 17 to 41%, demonstrating high reproducibility for drug susceptibility assays using both HIV-

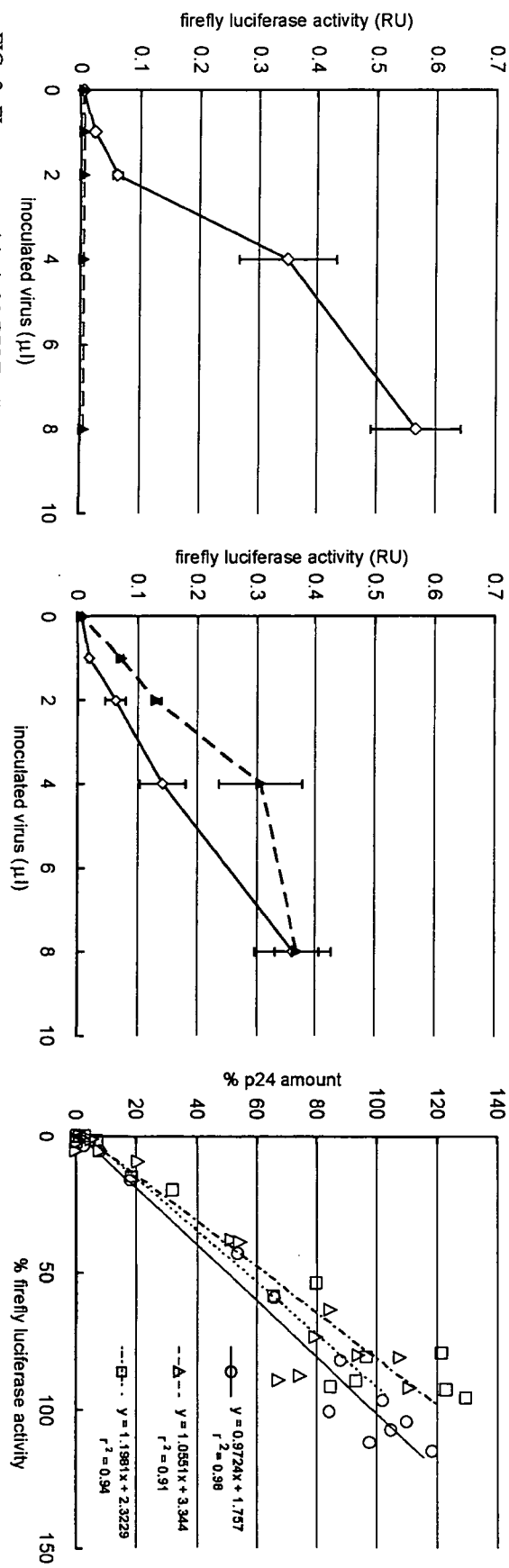

FIG. 2. FL reporter activity in MaRBLE cells accurately represents viral production\chatn. (a) X4-MaRBLE cells are susceptible to HXB2 (X4-tropic) but not JRCSF (R5-tropic) viruses. FL activity was confirmed as a reliable measure of X4-tropic HIV-1 in X4-MaRBLE cells by inoculating the cells with various amounts of HXB2 or JRCSF and reading FL activity 7 days later. Solid and dashed lines indicate HXB2 and JRCSF, respectively. (b) R5-MaRBLE cells are susceptible to both HXB2 (X4-tropic) and JRCSF (R5-tropic) viruses. FL activity was confirmed as a reliable measure of X4- and R5-tropic HIV-1 in R5-MaRBLE cells by inoculating the cells with various amounts of HXB2 or JRCSF and reading FL activity 7 days later. Solid and dashed lines indicate HXB2 and JRCSF, respectively. (c) FL activity and the amount of capsid antigen p24 are correlated in HIV-infected MaRBLE cells. The reliability of using FL activity instead of the amount of p24 to quantify HIV-1 production was evaluated by measuring intracellular FL activity and the amount of p24 antigen in the supernatant from the same culture. Solid, dashed, and dotted lines indicate HXB2-infected X4-MaRBLE cells, HXB2-infected R5-MaRBLE cells, and JRCSF-infected R5-MaRBLE cells, respectively. Percentages of FL activity and of p24 production were calculated from the following formula: percentage = (observed value with the drug − background value)/(observed value without the drug − background value) × 100. RU, relative units.

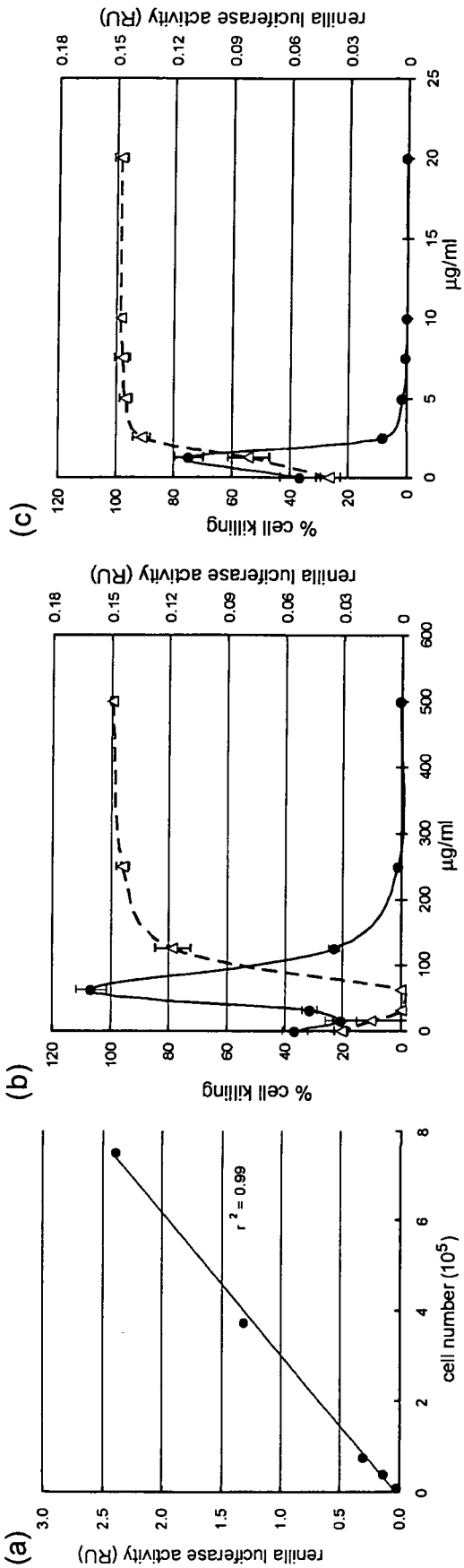

FIG. 3. Constitutively expressed RL in MaRBLE cells provides a reliable measure of cell number and viability. (a) RL activity accurately indicates MaRBLE cell numbers. The validity of using RL activity to monitor MaRBLE cell numbers was evaluated by measuring RL activity in various numbers of cells and plotting the corresponding values. RL activity and cell number were positively and linearly correlated ($r^2 = 0.99$). (b and c) RL activity reliably indicates hygromycin B and blasticidin S cytotoxicity in MaRBLE cells. The reliability of RL activity as a marker of cytotoxicity was evaluated for hygromycin B (b) and blasticidin S HCl (c). Cells were cultured for 1 week with serial dilutions of each drug and lysed, and their RL activities were determined. In graphs in both panels b and c, solid lines represent the RL activities of cell lysates and dashed lines indicate percentages of dead cells as determined by trypan blue staining. RU, relative units.

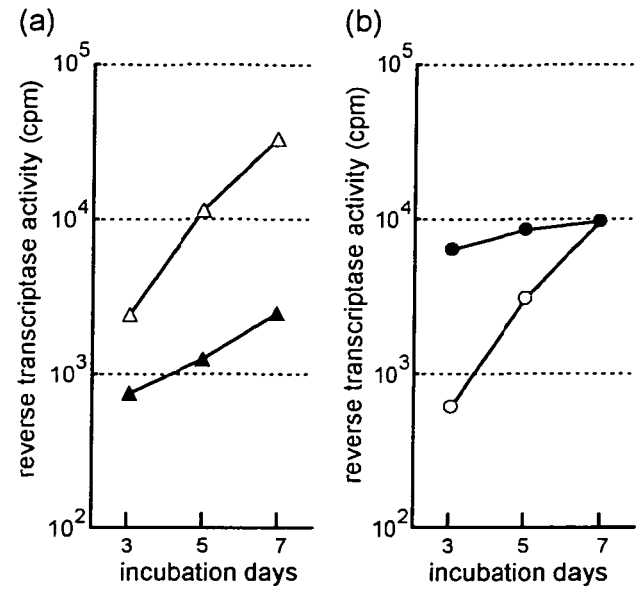

FIG. 4. Clinically derived isolates replicate in R5-MaRBLE cells as efficiently as in PBMC. The replication kinetics of two clinical isolates, 8 and 9, were compared after inoculation into both R5-MaRBLE cells and human PBMC. (a) Replication kinetics of isolate 8. Open and closed triangles indicate kinetics in R5-MaRBLE cells and PBMC, respectively. (b) Replication kinetics of isolate 9. Open and closed circles indicate kinetics in R5-MaRBLE cells and PBMC, respectively. cpm, counts per minute.

1-inoculated X4- and R5-MaRBLE cells. Interestingly, while the efavirenz and lopinavir susceptibilities of wild-type HXB2 were identical in evaluations with both X4- and R5-MaRBLE cells, the IC_{50}s for HXB2 and JRCSF were significantly different ($P < 0.001$) in the R5-MaRBLE cell line. Thus, in our assay, JRCSF appeared to be more susceptible than the HXB2 HIV-1 strain to efavirenz and slightly less resistant to lopinavir.

Drug susceptibility of drug-resistant HIV-1 can be evaluated using X4- and R5-MaRBLE cell lines. Given the accuracy and reproducibility of assays using MaRBLE cells to determine the drug susceptibilities of wild-type HXB2 and JRCSF, we then evaluated the reliability of using the cell lines for drug resistance phenotyping. Recombinant viruses with representative drug resistance mutations were constructed, and the drug resistance levels of the viruses were determined using X4-MaRBLE cells. The drug resistance levels associated with five patterns of nucleoside RT inhibitor (NRTI) resistance mutations are summarized in Table 2. Of the five mutant viral clones tested, four showed significant resistance to zidovudine, with resistance levels in the following order from lowest to highest: M41L/M184V/T215Y ≤ D67N/K70R < M41L/T215Y < M41L/D67N/K70R/T215Y. Thus, zidovudine resistance increased with the accumulation of thymidine analogue mutations (TAMs), and the M184V mutation caused reversion to the zidovudine resistance phenotype in the M41L/T215Y mutant, with a change in the susceptibility level of 12.5- to 3.5-fold relative to that of the wild-type virus, similar to results in previous reports (11, 19). Two clones with the M184V mutation demonstrated over 500-fold (>533.7- and >1,339.3-fold)-greater resistance to lamivudine but no significant resistance to didanosine and zalcitabine, although M184V has been re-

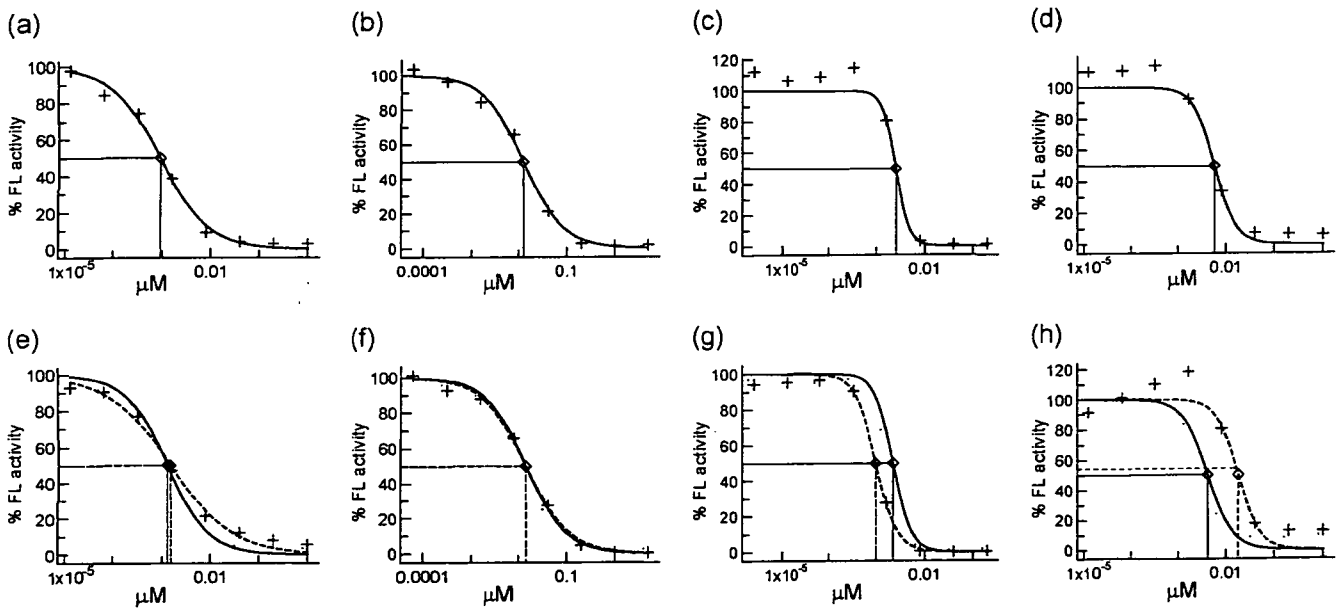

FIG. 5. Results of assays for HIV-1 drug susceptibility with MaRBLE reporter cell lines are highly reproducible. Dose-response curves for four representative agents against wild-type HXB2 and JRCSF are shown. Solid and dotted lines indicate HXB2 and JRCSF, respectively. (a to d) Results of assays for susceptibility to zidovudine, lamivudine, efavirenz, and lopinavir, respectively, using X4-MaRBLE cells. (e to h) Results of assays for susceptibility to zidovudine, lamivudine, efavirenz, and lopinavir, respectively, using R5-MaRBLE cells. The percentage of inhibition was calculated as follows: percentage = (observed FL activity with the drug − background FL activity)/(FL activity without the drug − background FL activity) × 100.

ported to confer a three- to fivefold increase in the level of resistance (14). Our data confirm the recent revalidation of using didanosine for cases involving the M184V mutation (39). Low-level but significant stavudine resistance in M41L/T215Y (change, 2.2-fold), M41L/M184V/T215Y (change, 2.9-fold), and M41L/D67N/K70R/T215Y (change, 3.8-fold) was found, consistent with data from previous reports (22, 33). All five clones demonstrated significant resistance to abacavir. The highest resistance was observed in the M41L/M184V/T215Y mutant, consistent with findings in previous reports that TAMs with M184V reduce susceptibility to abacavir 10-fold (1).

The drug resistance levels associated with the two most common nonnucleoside RT inhibitor (NNRTI) resistance mutations (K103N and Y181C) are summarized in Table 3. The K103N mutant virus demonstrated reduced susceptibility to both nevirapine (change, 78.6-fold) and efavirenz (change, 54.7-fold), whereas the Y181C virus was resistant only to nevirapine (change, 47.5-fold) but remained susceptible to efavirenz (change, 1.5-fold).

The drug resistance levels of three PI-resistant mutant clones (M46I, V82T, and L90M) are summarized in Table 4. Clones with M46I and L90M mutations did not demonstrate significant resistance to any PI tested, except for nelfinavir, to which the L90M clone demonstrated low-level (change, 3.3-fold) resistance. The clone with the V82T mutation demonstrated low-level resistance to indinavir (change, 3.8-fold), nelfinavir (change, 5.4-fold), amprenavir (change, 2.9-fold), and lopinavir (change, 5.0-fold), consistent with results in previous reports (8). Thus, the drug susceptibilities of viruses with resistance mutations evaluated with the MaRBLE cell lines matched those from previous reports of drug resistance, indicating the reliability of using the new cell lines to evaluate drug resistance.

To assess the reliability of using R5-MaRBLE cells to evaluate the levels of drug resistance of viral isolates from patients for whom treatment failed, seven cases were selected and viruses were isolated by coculture with normal human PBMC. Among the isolates from these seven cases, isolate 7 did not yield measurable virus by coculture. Therefore, a protease-RT gene fragment was amplified by RT-PCR and inserted into the HXB2 backbone. As shown in Table 5, isolate 1 had three minor mutations in the protease region and the virus was susceptible to all four inhibitors tested. The increase in resistance, calculated by comparison to the drug resistance of JRCSF, was <1.0-fold for zidovudine, lamivudine, and lopina-

TABLE 1. Susceptibility of wild-type HXB2 and JRCSF to representative antiretrovirals as determined using X4- and R5-MaRBLE cells

Cell line	Agent	Mean IC_{50} (nM) ± SD (CV [%]) for[a]:		
		HXB2 (n = 18)	HXB2 (n = 21)	JRCSF (n = 24)
X4-MaRBLE	Zidovudine	0.9 ± 0.4 (41)		
	Lamivudine	12.3 ± 3.9 (32)		
	Efavirenz	2.7 ± 1.0 (37)		
	Lopinavir	6.0 ± 1.0 (17)		
R5-MaRBLE	Zidovudine		1.3 ± 0.4 (31)	1.5 ± 0.6 (40)
	Lamivudine		13.6 ± 4.8 (35)	13.4 ± 3.6 (27)
	Efavirenz		2.1 ± 0.5[b] (24)	1.0 ± 0.3[b] (30)
	Lopinavir		4.2 ± 1.4[b] (33)	17.6 ± 6.9[b] (39)

[a] n, number of isolates of the indicated virus strain.
[b] IC_{50}s of efavirenz and lopinavir were significantly different for HXB2 and JRCSF in R5-MaRBLE cells ($P < 0.001$).

TABLE 5. Susceptibilities of seven patient-derived viral isolates to representative drugs assayed using R5-MaRBLE cells

Strain or isolate (subtype)	Tropism[b]	RT mutation(s)	Protease mutation(s)	IC_{50} (nM) ± SD (change, *n*-fold) of:			
				Zidovudine	Lamivudine	Efavirenz	Lopinavir
JRCSF (B)	R5	None	L63P	1.4 ± 0.6 (1)	13.6 ± 4.6 (1)	0.9 ± 0.1 (1)	19.3 ± 8.4 (1)
1 (B)	R5	None	L63P/T, A71A/V, V77I	1.2 (0.7)	4.2 (0.3)	1.5 (1.8)	6.8 (0.5)
2 (B)	X4, R5	M41L, D67N, K70R, K101Q, M184V, L210L/W, T215F, K219Q	L10I, L33F, M46I, F53L, I54V, L63P, A71V, G73S/T, V77I, V82F, L90M	56.1 (32.9)	>5,000 (>380.7)	1.1 (1.3)	>1,000 (>76.5)
3 (F)	X4, R5	M41L, E44E/D, D67N, K101K/E, V118I, L210W, T215Y	K20T, D30N, M36I, M46M/L, L63P, A71V, N88D	195.1 (114.5)	34.5 (2.6)	0.1 (0.2)	ND[c] (ND)
4 (B)	X4, R5	M41L, E44A, D67N, V118I, L210W, T215Y	L10V, K20T, D30N, M36I, I54V, L63T, A71V, V77V/I, N88D, L90M	326.5 (191.7)	13.5 (1.0)	0.2 (0.2)	123.4 (9.4)
5 (B)	X4, R5	M41L, E44D, D67N, V118I, M184V, L210W, T215Y	L10V, K20R, V32I, M36I, M46L, F53F/L, I54V, L63P, A71V, V82A, L90M	177.4 (104.1)	>5,000 (>380.7)	0.5 (0.6)	986.8 (75.5)
6 (F)	R5	M41L, E44D, D67N, V118I, L210W, T215Y	L10I, K20T, M36I, M46I, F53L, L63L/I/T/P, A71V, I84V, L90M	381.7 (224.0)	88.0 (6.7)	0.3 (0.4)	190.6 (14.6)
7R[a] (B)	X4	K103N	L63C, V77I	2.1 (1.5)	22.3 (1.6)	60.2 (66.8)	7.6 (0.4)

[a] Recombinant HXB2 with patient-derived protease and RT sequences.
[b] The tropism of each virus was determined by using X4-GHOST and R5-GHOST cells.
[c] ND, not determined.

we could easily evaluate culture conditions and their effects on assay results.

These two characteristics confer a great advantage to using the MaRBLE cell lines for screening new antiretroviral agents. They allow both early- and late-phase inhibitor candidates to be evaluated under the same protocol, as the assay permits multiple viral replications. Moreover, monitoring of RL activity allows false-positive results (inhibition by test drugs due to cytotoxicity) to be detected and eliminated. Finally, the use of RL activity greatly improved the efficacy of screening.

The MaRBLE cell lines stably expressed the transfected genes, as confirmed by the stable expression of CD4, CXCR4, and CCR5 on the surfaces of cells maintained in culture for up to 6 months with continuous passage. We also confirmed that the two reporter genes were stably expressed and that IC_{50}s were identical for both newly plated and 6-month-old cultures (data not shown).

In conclusion, we successfully established two unique cell lines, X4-MaRBLE and R5-MaRBLE, which are useful for assaying viral drug resistance and for screening new antiretroviral compounds. Although the cost of phenotypic assays using our cell lines may be less than that of commercial systems, the assays require a biosafety level 3 laboratory, general culture equipment, and a luminometer for readout. Since these are all expensive items, the assay price should be reduced and the assay protocol should be simplified for wider usage of the assay.

ACKNOWLEDGMENTS

We thank Hiroshi Yoshikura, Mari Takizawa, and Mitsuo Honda for their help and discussions. We also thank Claire Baldwin for her help in preparing the manuscript.

This study was supported by a grant from the Human Sciences Foundation and the Program for Promotion of Fundamental Studies in Health Sciences of the National Institute of Biomedical Innovation (NIBIO).

REFERENCES

1. **Ait-Khaled, M., A. Rakik, P. Griffin, A. Cutrell, M. A. Fischl, N. Clumeck, S. B. Greenberg, R. Rubio, B. S. Peters, F. Pulido, J. Gould, G. Pearce, W. Spreen, M. Tisdale, and S. Lafon.** 2002. Mutations in HIV-1 reverse transcriptase during therapy with abacavir, lamivudine and zidovudine in HIV-1-infected adults with no prior antiretroviral therapy. Antivir. Ther. 7:43–51.
2. **Baxter, J. D., D. L. Mayers, D. N. Wentworth, J. D. Neaton, M. L. Hoover, M. A. Winters, S. B. Mannheimer, M. A. Thompson, D. I. Abrams, B. J. Brizz, J. P. Ioannidis, T. C. Merigan, et al.** 2000. A randomized study of antiretroviral management based on plasma genotypic antiretroviral resistance testing in patients failing therapy. AIDS 14:F83–93.
3. **Bento, F. M., D. Takeshita, C. B. Sacramento, T. R. Machado, M. B. Mathor, A. K. Carmona, and S. W. Han.** 2004. Over expression of the selectable marker blasticidin S deaminase gene is toxic to human keratinocytes and murine BALB/MK cells. BMC Biotechnol. 4:29.
4. **Bosch, R. J., G. F. Downey, D. A. Katzenstein, N. Hellmann, L. Bacheler, and M. A. Albrecht.** 2003. Evaluation of cutpoints for phenotypic hypersusceptibility to efavirenz. AIDS 17:2395–2396.
5. **Cingolani, A., A. Antinori, M. G. Rizzo, R. Murri, A. Ammassari, F. Baldini, S. Di Giambenedetto, R. Cauda, and A. De Luca.** 2002. Usefulness of monitoring HIV drug resistance and adherence in individuals failing highly active antiretroviral therapy: a randomized study (ARGENTA). AIDS 16:369–379.
6. **Clevenbergh, P., J. Durant, P. Halfon, P. del Giudice, V. Mondain, N. Montagne, J. M. Schapiro, C. A. Boucher, and P. Dellamonica.** 2000. Persisting long-term benefit of genotype-guided treatment for HIV-infected patients failing HAART. The Viradapt Study: week 48 follow-up. Antivir. Ther. 5:65–70.
7. **Cohen, C. J., S. Hunt, M. Sension, C. Farthing, M. Conant, S. Jacobson, J. Nadler, W. Verbiest, K. Hertogs, M. Ames, A. R. Rinehart, and N. M. Graham.** 2002. A randomized trial assessing the impact of phenotypic resistance testing on antiretroviral therapy. AIDS 16:579–588.
8. **Condra, J. H., W. A. Schleif, O. M. Blahy, L. J. Gabryelski, D. J. Graham, J. C. Quintero, A. Rhodes, H. L. Robbins, E. Roth, M. Shivaprakash, D. Titus, T. Yang, H. Teppler, K. E. Squires, P. J. Deutsch, and E. A. Emini.** 1995. In vivo emergence of HIV-1 variants resistant to multiple protease inhibitors. Nature 374:569–571.
9. **Durant, J., P. Clevenbergh, P. Halfon, P. Delgiudice, S. Porsin, P. Simonet, N. Montagne, C. A. Boucher, J. M. Schapiro, and P. Dellamonica.** 1999. Drug-resistance genotyping in HIV-1 therapy: the VIRADAPT randomised controlled trial. Lancet 353:2195–2199.
10. **Eshleman, S. H., G. Crutcher, O. Petrauskene, K. Kunstman, S. P. Cunningham, C. Trevino, C. Davis, J. Kennedy, J. Fairman, B. Foley, and J. Kop.** 2005. Sensitivity and specificity of the ViroSeq human immunodefi-

ciency virus type 1 (HIV-1) genotyping system for detection of HIV-1 drug resistance mutations by use of an ABI PRISM 3100 genetic analyzer. J. Clin. Microbiol. 43:813–817.
11. **Fumero, E., and D. Podzamczer.** 2003. New patterns of HIV-1 resistance during HAART. Clin. Microbiol. Infect. 9:1077–1084.
12. **Gervaix, A., D. West, L. M. Leoni, D. D. Richman, F. Wong-Staal, and J. Corbeil.** 1997. A new reporter cell line to monitor HIV infection and drug susceptibility in vitro. Proc. Natl. Acad. Sci. USA 94:4653–4658.
13. **Grant, R. M., D. R. Kuritzkes, V. A. Johnson, J. W. Mellors, J. L. Sullivan, R. Swanstrom, R. T. D'Aquila, M. Van Gorder, M. Holodniy, R. M. Lloyd Jr., C. Reid, G. F. Morgan, and D. L. Winslow.** 2003. Accuracy of the TRUGENE HIV-1 genotyping kit. J. Clin. Microbiol. 41:1586–1593.
14. **Gu, Z., Q. Gao, X. Li, M. A. Parniak, and M. A. Wainberg.** 1992. Novel mutation in the human immunodeficiency virus type 1 reverse transcriptase gene that encodes cross-resistance to 2',3'- dideoxyinosine and 2',3'-dideoxycytidine. J. Virol. 66:7128–7135.
15. **Hachiya, A., S. Aizawa-Matsuoka, M. Tanaka, Y. Takahashi, S. Ida, H. Gatanaga, Y. Hirabayashi, A. Kojima, M. Tatsumi, and S. Oka.** 2001. Rapid and simple phenotypic assay for drug susceptibility of human immunodeficiency virus type 1 using CCR5-expressing HeLa/CD4(+) cell clone 1–10 (MAGIC-5). Antimicrob. Agents Chemother. 45:495–501.
16. **Hartley, J. W., and W. P. Rowe.** 1976. Naturally occurring murine leukemia viruses in wild mice: characterization of a new "amphotropic" class. J. Virol. 19:19–25.
17. **Hertogs, K., M. P. de Bethune, V. Miller, T. Ivens, P. Schel, A. Van Cauwenberge, C. Van Den Eynde, V. Van Gerwen, H. Azijn, M. Van Houtte, F. Peeters, S. Staszewski, M. Conant, S. Bloor, S. Kemp, B. Larder, and R. Pauwels.** 1998. A rapid method for simultaneous detection of phenotypic resistance to inhibitors of protease and reverse transcriptase in recombinant human immunodeficiency virus type 1 isolates from patients treated with antiretroviral drugs. Antimicrob. Agents Chemother. 42:269–276.
18. **Hollinger, F. B., J. W. Bremer, L. E. Myers, J. W. Gold, L. McQuay, and the NIH/NIAID/DAIDS/ACTG Virology Laboratories.** 1992. Standardization of sensitive human immunodeficiency virus coculture procedures and establishment of a multicenter quality assurance program for the AIDS Clinical Trials Group. J. Clin. Microbiol. 30:1787–1794.
19. **Imamichi, T.** 2004. Action of anti-HIV drugs and resistance: reverse transcriptase inhibitors and protease inhibitors. Curr. Pharm. Des. 10:4039–4053.
20. **Johnson, V. A., F. Brun-Vezinet, B. Clotet, B. Conway, D. R. Kuritzkes, D. Pillay, J. M. Schapiro, A. Telenti, and D. D. Richman.** 2005. Update of the drug resistance mutations in HIV-1: fall 2005. Top. HIV Med. 13:125–131.
21. **Kimpton, J., and M. Emerman.** 1992. Detection of replication-competent and pseudotyped human immunodeficiency virus with a sensitive cell line on the basis of activation of an integrated beta-galactosidase gene. J. Virol. 66:2232–2239.
22. **Larder, B. A., S. D. Kemp, and P. R. Harrigan.** 1995. Potential mechanism for sustained antiretroviral efficacy of AZT-3TC combination therapy. Science 269:696–699.
23. **Larder, B. A., A. Kohli, P. Kellam, S. D. Kemp, M. Kronick, and R. D. Henfrey.** 1993. Quantitative detection of HIV-1 drug resistance mutations by automated DNA sequencing. Nature 365:671–673.
24. **Miyake, H., Y. Iizawa, and M. Baba.** 2003. Novel reporter T-cell line highly susceptible to both CCR5- and CXCR4-using human immunodeficiency virus type 1 and its application to drug susceptibility tests. J. Clin. Microbiol. 41:2515–2521.
25. **Myint, L., M. Matsuda, Z. Matsuda, Y. Yokomaku, T. Chiba, A. Okano, K. Yamada, and W. Sugiura.** 2004. Gag non-cleavage site mutations contribute to full recovery of viral fitness in protease inhibitor-resistant human immunodeficiency virus type 1. Antimicrob. Agents Chemother. 48:444–452.
26. **Petropoulos, C. J., N. T. Parkin, K. L. Limoli, Y. S. Lie, T. Wrin, W. Huang, H. Tian, D. Smith, G. A. Winslow, D. J. Capon, and J. M. Whitcomb.** 2000. A novel phenotypic drug susceptibility assay for human immunodeficiency virus type 1. Antimicrob. Agents Chemother. 44:920–928.
27. **Reed, L., and H. Muench.** 1938. A simple method of estimating fifty percent endpoint. Am. J. Hyg. 27:493–497.
28. **Sarkar, G., and S. S. Sommer.** 1990. The "megaprimer" method of site-directed mutagenesis. BioTechniques 8:404–407.
29. **Shimizu, Y. K., R. H. Purcell, and H. Yoshikura.** 1993. Correlation between the infectivity of hepatitis C virus in vivo and its infectivity in vitro. Proc. Natl. Acad. Sci. USA 90:6037–6041.
30. **Shulman, N. S., R. J. Bosch, J. W. Mellors, M. A. Albrecht, and D. A. Katzenstein.** 2004. Genetic correlates of efavirenz hypersusceptibility. AIDS 18:1781–1785.
31. **Spenlehauer, C., C. A. Gordon, A. Trkola, and J. P. Moore.** 2001. A luciferase-reporter gene-expressing T-cell line facilitates neutralization and drug-sensitivity assays that use either R5 or X4 strains of human immunodeficiency virus type 1. Virology 280:292–300.
32. **Sugden, B., K. Marsh, and J. Yates.** 1985. A vector that replicates as a plasmid and can be efficiently selected in B-lymphoblasts transformed by Epstein-Barr virus. Mol. Cell. Biol. 5:410–413.
33. **Tisdale, M., S. D. Kemp, N. R. Parry, and B. A. Larder.** 1993. Rapid in vitro selection of human immunodeficiency virus type 1 resistant to 3'-thiacytidine inhibitors due to a mutation in the YMDD region of reverse transcriptase. Proc. Natl. Acad. Sci. USA 90:5653–5656.
34. **Tural, C., L. Ruiz, C. Holtzer, J. Schapiro, P. Viciana, J. Gonzalez, P. Domingo, C. Boucher, C. Rey-Joly, and B. Clotet.** 2002. Clinical utility of HIV-1 genotyping and expert advice: the Havana trial. AIDS 16:209–218.
35. **Vandamme, A. M., F. Houyez, D. Banhegyi, B. Clotet, G. De Schrijver, K. A. De Smet, W. W. Hall, R. Harrigan, N. Hellmann, K. Hertogs, C. Holtzer, B. Larder, D. Pillay, E. Race, J. C. Schmit, R. Schuurman, E. Schulse, A. Sonnerborg, and V. Miller.** 2001. Laboratory guidelines for the practical use of HIV drug resistance tests in patient follow-up. Antivir. Ther. 6:21–39.
36. **Vodros, D., C. Tscherning-Casper, L. Navea, D. Schols, E. De Clercq, and E. M. Fenyo.** 2001. Quantitative evaluation of HIV-1 coreceptor use in the GHOST3 cell assay. Virology 291:1–11.
37. **Willey, R. L., R. Shibata, E. O. Freed, M. W. Cho, and M. A. Martin.** 1996. Differential glycosylation, virion incorporation, and sensitivity to neutralizing antibodies of human immunodeficiency virus type 1 envelope produced from infected primary T-lymphocyte and macrophage cultures. J. Virol. 70:6431–6436.
38. **Wilson, J. W.** 2003. Update on antiretroviral drug resistance testing: combining laboratory technology with patient care. AIDS Read. 13:25–30, 35–38.
39. **Winters, M. A., R. J. Bosch, M. A. Albrecht, and D. A. Katzenstein.** 2003. Clinical impact of the M184V mutation on switching to didanosine or maintaining lamivudine treatment in nucleoside reverse-transcriptase inhibitor-experienced patients. J. Infect. Dis. 188:537–540.
40. **Yoshikura, H.** 1989. Thermostability of human immunodeficiency virus (HIV-1) in a liquid matrix is far higher than that of an ecotropic murine leukemia virus. Jpn. J. Cancer Res. 80:1–5.

Parasite Immunology, 2008, 30, 13–21 DOI: 10.1111/j.1365-3024.2007.00988.x

Recognition profiles of microsporidian *Encephalitozoon cuniculi* polar tube protein 1 with human immunoglobulin M antibodies

K. FURUYA,[1] M. OMURA,[1] S. KUDO,[2] W. SUGIURA[3] & H. AZUMA[4]

[1]Department of Parasitology, National Institute of Infectious Diseases, Tokyo, Japan, [2]Hokkaido Institute of Public Health, Sapporo, Japan, [3]AIDS Research Center, National Institute of Infectious Diseases, Tokyo, Japan, [4]Hokkaido Red Cross Blood Center, Sapporo, Japan

SUMMARY

Microsporidian Encephalitozoon cuniculi *has a unique organelle called a polar tube (PT), the extrusion of which is absolutely required to invade a host cell. We recently detected anti-*E. cuniculi *PT immunoglobulin (Ig) M antibodies in sera from many healthy individuals. The present one-dimensional (1-D) immunoblot analysis predominantly detected a band at 52 kDa in all of the examined human sera with anti-PT IgM. The use of mouse monoclonal antibody confirmed that the 52-kDa band detected in 1-D immunoblots was an antigen derived from the PT, which represents a glycoprotein nature. In addition, from changes in the immunoreactivity of the 52-kDa band before and after treatment with NaOH, we determined that the 24 human serum samples with anti-PT IgM activities could be roughly grouped into three types: (i) sera containing antibodies against only a saccharic determinant (*n = *3); (ii) sera containing antibodies against only a proteinic determinant (*n = *11); and (iii) sera showing dual recognition of saccharic and proteinic determinants (*n = *10). Further two-dimensional (2-D) immunoblot analysis followed by proteomic analysis confirmed that human sera with anti-PT IgM reacted with* E. cuniculi *polar tube protein 1 (PTP1). Such circulating IgM antibodies may be important in the first line of defence against* E. cuniculi *infection.*

Keywords *antigenic determinant,* Encephalitozoon cuniculi, *human IgM antibody, Microsporidia, polar tube*

INTRODUCTION

Encephalitozoon cuniculi is a spore-forming obligate intracellular parasitic pathogen belonging to the phylum Microsporidia (1); it can also be a zoonotic parasite (2). Various animals can be naturally infected by *E. cuniculi* and humans can also be affected by this pathogen (3). However, most *E. cuniculi* infections occur in human immunodeficiency virus (HIV)-infected immunocompromised patients (2,4). A few cases of *E. cuniculi* infection have also been reported in transplant patients (2,5,6). Apart from an accidentally infected French individual who had severe keratoconjunctivitis (7), no symptomatic cases of infection with *E. cuniculi* among immunocompetent persons have been described (2,4). Thus, it is most unlikely that *E. cuniculi* causes microsporidiosis in immunocompetent persons (2,4). In humans, it can be regarded as an opportunistic pathogen (8,9).

We recently demonstrated immunoglobulin (Ig) M antibodies against the polar tubes (PTs) of *E. cuniculi* in about 36% of healthy people in Japan (10); by contrast, such IgM antibodies were poorly detected among HIV-positive persons. The rate of positivity for anti-PT IgM was significantly reduced with increasing age and decreasing CD4 cell count. These seroepidemiological results clearly indicate that circulating anti-PT IgM antibodies that are capable of strongly reacting with filaments extruded from germinated spores exist, thus suggesting that such antibodies may play a part in protective immunity.

The main objectives of this study were to provide further information about the immunoreactivity of human anti-PT IgM and to identify the corresponding determinants using one-dimensional (1-D) and two-dimensional (2-D) immunoblot analyses, and other biochemical and proteomic means.

MATERIALS AND METHODS

Serum samples

Twenty-four human serum samples were used for this study. These samples were collected from healthy individuals

Correspondence: K. Furuya, Department of Parasitology, National Institute of Infectious Diseases, 1-23-1 Toyama, Shinjuku-ku, Tokyo 162-8640, Japan (e-mail: kfuruya@nih.go.jp).
Received: 17 July 2007
Accepted for publication: 14 September 2007

under the ethical considerations described in a previous study (10).

As the positive control, serum samples from 11 infected rabbits were also used for this study. All the rabbits were sacrificed after approval from the breeding owners and were microbiologically confirmed to carry the pathogen in organs such as the brain and kidney. Isolated *E. cuniculi* spores from the organs were identified by polymerase chain reaction, as described before (11). The internal transcribed spacer gene sequence revealed that the *E. cuniculi* isolates were all classified into genotype 1.

In addition, 11 normal rabbit serum samples, which were serologically negative, were used as the negative control.

Mouse monoclonal antibody

A mouse monoclonal antibody against the soluble antigen of *E. cuniculi* PTs was generated using a hybridoma technique (12), which was tentatively named MAb2 for this study. After the second cloning, culture supernatants containing MAb2 were employed in the present study. In a later study, monoclonal antibodies from mouse ascitic fluids were available and were classified as IgE (manuscript in preparation). To detect IgE in this study, we used goat anti-mouse IgG + M + A (H + L) and rabbit anti-mouse IgG (H + L), which were labelled with enzyme, as documented below. All the reagents used could detect IgE, since they are also specific for light chains.

Preparation of purified spores of *Encephalitozoon cuniculi*

Encephalitozoon cuniculi spores of strain HF (genotype 1) were collected from the culture supernatants of infected RK 13 cells and purified using Percoll gradient centrifugation, as described previously (10). Finally, separated spores were filtered through Ultrafree-MC membranes (5·0 μm; Millipore Corporation, Bedford, MA).

Enzyme-linked immunosorbent assay (ELISA)

As described in a previous paper (10), anti-*E. cuniculi* PT antibodies were measured using a 96-well flat-bottom microplate coated with germinated spores. Twofold dilutions of each serum sample, starting a 1 : 50 dilution, were tested; bound antibodies were detected by the secondary antibody labelled with peroxidase (PO). Signals of PO bound to human or animal antibodies were visualized using an aminoethyl carbazole substrate kit (Zymed Laboratories Inc., San Diego, CA). The following PO conjugates were used as the secondary antibodies: rabbit anti-human IgM (μ-chain specific; QED Bioscience, San Diego, CA) for human IgM; goat anti-mouse IgG + M + A (H + L; Zymed Laboratories) for mouse monoclonal antibody. Also, protein A/G-PO conjugate (Prozyme Inc., San Leandro, CA) and protein A-PO conjugate (Kirkegaard & Perry Laboratories, Gaithersburg, MD) were used for detecting human IgG and rabbit IgG, respectively. Dilutions of the second reagents were adjusted between 1 : 3000 and 1 : 5000.

1-D polyacrylamide gel electrophoresis (1-D PAGE)

Purified *E. cuniculi* spores were suspended in an appropriate volume of Laemmli sample buffer (Bio-Rad Laboratories, Hercules, CA) containing 5% 2-mercaptoethanol (Bio-Rad) and heated at 95°C for 5 min. After centrifugation at about 7800 *g* for 5 min, pellets were treated twice more with the same buffer and the three supernatants were pooled. The protein fraction of these pooled supernatants was desalted using a NAP-5 column (GE Healthcare Bio-Sciences AB, Uppsala, Sweden). This soluble protein fraction was used as an antigen for 1-D immunoblot analysis.

Approximately 60 μg of the microsporidial soluble fraction was electrophoresed vertically using 15% polyacrylamide Ready mini-gels (Bio-Rad) under reducing conditions.

1-D immunoblot analysis

Electrophoresed spore proteins separated by 1-D PAGE were transferred electrically onto polyvinylidene fluoride (PVDF) membranes (immobilon transfer membranes; Millipore Corporation). Blotted membranes were cut into strips of about 4-mm width. Half of the strips were treated with a 0·055 M NaOH solution for 16 h at 40°C to remove carbohydrate chains from glycoproteins, according to the method described by Duk *et al.* (13). NaOH-treated strips were washed extensively with pure water.

All of the strips to be tested were treated with blocking buffer (SuperBlock; Pierce Chemical Company, Rockford, IL) and subsequently incubated with human sera, rabbit sera or a culture supernatant containing MAb2. Dilutions of human sera, rabbit sera and the supernatant to be tested were 1 : 100. Secondary antibodies labelled with alkaline phosphatase (ALP) were used to detect primary antibodies: goat anti-human IgM (μ-chain specific; Kirkegaard & Perry Laboratories) for human IgM; goat anti-rabbit IgM (μ-chain specific; Southern Biotechnology Associates, Birmingham, AL) for rabbit IgM; rabbit anti-mouse IgG (H + L; Zymed Laboratories) for mouse monoclonal antibody. The secondary antibodies were used at dilutions of 1 : 1000–1 : 3000. Reactions with the primary antibodies and the secondary antibodies were performed for 90 min at room temperature with shaking. After extensive washing with phosphate-buffered saline containing 0·05% Tween 20 (PBS-T), antibody binding was detected using a BCIP/

NBT phosphatase substrate kit (Kirkegaard & Perry Laboratories).

For each human serum, mouse monoclonal antibody and rabbit serum, the change in immunoreactivity between a NaOH-treated strip and an untreated strip was observed. In addition, the participation of a saccharic determinant in an immunological reaction was determined.

Analysis of lectin–carbohydrate interactions

Using some of the NaOH-treated or NaOH-untreated strips described above, the reactivities of various biotinylated lectins were tested. For this test, a biotinylated lectin kit I (BK-1000; Vector Laboratories, Buringame, CA), containing concanavalin A (ConA), *Dolichos biflorus* agglutinin, peanut agglutinin, *Ricinus communis* agglutinin I, soybean agglutinin, *Ulex europaeus* agglutinin I and wheat germ agglutinin, was used. Blots were incubated in a 20 μg/mL solution of each biotinylated lectin, in accordance with the manufacturer's instructions, followed by a 1 : 5000 dilution of streptavidin–ALP conjugate (Molecular Probes Inc., Eugene, OR). A BCIP/NBT phosphatase substrate kit (Kirkegaard & Perry Laboratories) was employed for colour development.

2-D polyacrylamide gel electrophoresis (2-D PAGE)

To an approximately 5×10^8 spore pellet, a 5% sodium dodecyl sulphate (SDS) solution was added, and the suspension was boiled for 5 min. Proteins were precipitated by the addition of trichloroacetic acid at a final concentration of 10%, washed once with cold 90% acetone, and dissolved in sample buffer containing 8 M urea, 2% CHAPS, 1% 1,4-dithiothreitol (DTT; Wako Pure Chemical Industries, Osaka, Japan), and 0·5% Pharmalyte (pH 3–10; Amersham Biosciences AB, Uppsala, Sweden). To remove protein aggregates, the protein solution was centrifuged and the supernatants were used as samples for 2-D PAGE. Protein concentrations were measured using a 2D-Quant kit (Amersham).

Isoelectric focusing was performed using commercially available Immobiline DryStrip gels (7 cm, pH 3–10; Amersham). Samples (about 50 μg of spore protein) were loaded by rehydration for 15 h in a solution containing 8 M urea, 2% CHAPS, 1% DTT and 0·5% Pharmalyte (pH 3–10). Isoelectric focusing was performed using an Ettan IPGphor II IEF system (Amersham) for 11 519 Vh. Voltage profiles were chosen according to the manual provided with the system. After consecutive equilibration of gels in a 50 mM Tris–HCl (pH 8·8) solution containing 6 M urea, 30% glycerol, 2% SDS and 1% DTT for 15 min, separation in the second dimension was performed using a mini-gel (10 × 10 cm) electrophoresis system with 12·5% Ready gels (Biocraft Inc., Tokyo, Japan), at 20 mA/gel.

N-terminal peptide sequencing

After 2-D PAGE, blotted proteins were stained with BODIPY FL-X, SE (Molecular Probes). Protein spots corresponding to those recognized by serum samples were excised and subjected to N-terminal sequence analysis in a Procise 494 protein sequencer (Applied Biosystems, Foster City, CA). Edman degradation was performed according to a standard program supplied by Applied Biosystems. The amino acid sequences obtained were compared to those of known proteins in the GenomeNet BLAST2 NR-AA database using the Web-accessible FASTA search program.

LC-MS/MS analysis

Spots assigned to immunogenic proteins were also excised from 2-D gels as described above. Gel pieces were subjected to in-gel digestion using the procedure published by Hellman *et al.* (14). Briefly, the protein in each gel plug was reduced with 100 mM DTT for 30 min at 50°C, alkylated with 100 mM iodoacetamide (Wako Pure Chemical) for 30 min at 37°C, and digested with 25 ng/μL trypsin (Wako Pure Chemical) overnight at 37°C. Peptides were extracted from the gel by diffusion in a 50% acetonitrile solution containing 5% formic acid, vacuum-dried, and then reconstituted in 20 μL of 0·1% trifluoroacetic acid. Extracted peptides were loaded on a high-performance liquid chromatography system (LC; MAGIC2002, Michrom BioResources Co. Ltd, Auburn, CA), eluted using an acetic acid–acetonitrile gradient, and directly injected into an LCQ ion trap mass spectrometer (MS; LCQ-Deca XP, Thermo Electron Co. Ltd, San Jose, CA) fitted with a nanoelectrospray ionization source, and operated in the positive ion mode. MS/MS spectra were acquired using data-dependent scanning, processed using the SEQUEST software program, and then searched against the NCBI NR database.

2-D immunoblot analysis

Spore proteins separated by 2-D PAGE were transferred onto PVDF membranes (ProBlot membranes, Applied Biosystems). Blotted membranes were treated with blocking buffer (SuperBlock) overnight at 4°C. Representative human sera were used as primary antibodies at a dilution of 1 : 100. ALP-labelled anti-human IgM (μ-chain specific; Kirkegaard & Perry Laboratories) was used as a secondary antibody at a dilution of 1 : 1000. Reactions with the primary and secondary antibodies were performed for 2 and 1 h, respectively, at room temperature with shaking. After extensive washing with

Journal compilation © 2007 Blackwell Publishing Ltd, *Parasite Immunology*, 30, 13–21

PBS-T, antibody binding was detected using a BCIP/NBT phosphatase substrate kit (Kirkegaard & Perry Laboratories).

As a positive control, we used a pool of 11 sera from infected rabbits at a dilution of 1 : 400. In addition, a pool of 11 sera from normal rabbits was used as a negative control at the same dilution. A culture supernatant containing MAb2 monoclonal antibody was also used at a dilution of 1 : 100 for epitope analysis. To detect these primary antibodies, ALP-labelled protein A (Zymed Laboratories) and ALP-labelled rabbit anti-mouse IgG (H + L; Zymed Laboratories) were used for rabbit IgG and the monoclonal antibody, respectively, at a dilution of 1 : 1000.

RESULTS

Measurements of anti-PT antibodies in the ELISA test

Twenty-four human serum samples used for this study revealed anti-PT IgM activities at titres between 1 : 200 and 1 : 1600 in the ELISA test. Figure 1(a) shows filaments that are strongly immunostained with IgM antibodies in the serum H-168. All samples except for H-197 had IgG antibody activity for extruded filaments below 1 : 50. However, the positive signal of H-197 was very weak, even at lower dilutions, probably because of the use of protein A/G conjugate as a secondary antibody.

Figure 1(b) shows filaments immunostained with IgG antibodies in a rabbit serum, which was used as a positive control for ELISA testing. The culture supernatant showed monoclonal antibody (MAb2) weakly immunostained filaments when it was tested by ELISA (data not shown).

Immunoreactivity of human sera on 1-D blots before and after treatment with NaOH

All 24 human serum samples generated clearly positive signals of an IgM antibody on a band migrating at 52 kDa in the 1-D immunoblot analysis without NaOH treatment (Figure 2; odd-numbered strips). Besides the positive signals for this 52-kDa band, which was MAb2-positive (strip P1), most sera also reacted with some bands below 52 kDa; however, the extent of staining was very weak, especially in bands below 28 kDa.

Using the 24 human serum samples, changes in IgM antibody binding were examined on 1-D blots before and after treatment with NaOH. When 1-D blots treated with NaOH were used for testing, the same human sera were divided into three groups based on the degree of immunostaining of the 52-kDa band: (i) 11 sera showed almost unchanged antibody binding (Figure 2; strips 6, 8 and 10); (ii) three sera showed no antibody binding (Figure 2; strips 2 and 4); and (iii) 10 sera showed significantly reduced antibody binding, resulting in the formation of faint or thin bands (Figure 2; strips 12, 14 and 16).

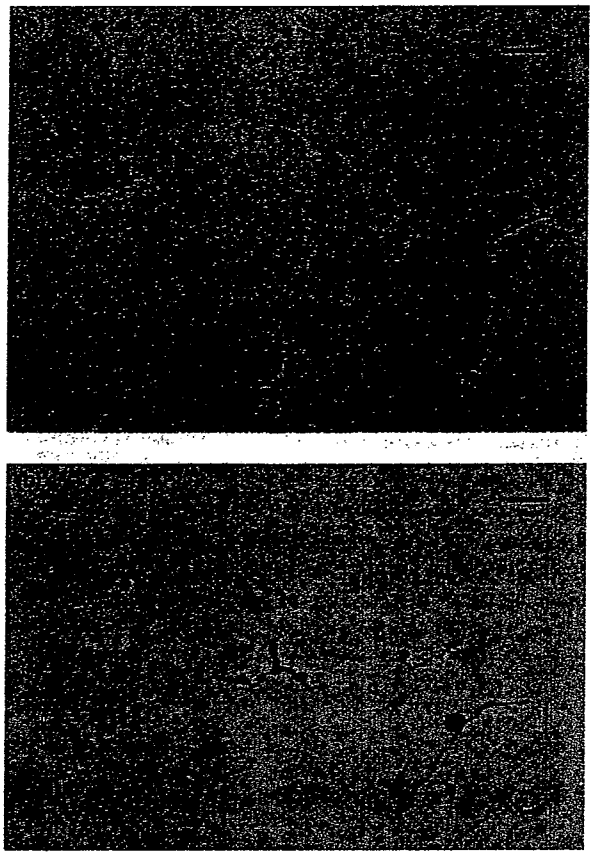

Figure 1 Immunostaining of filaments (PTs) that extruded from *E. cuniculi*-germinated spores with human IgM antibodies or rabbit IgG antibodies. (a) Positive results obtained by a 1 : 200 dilution of H-168 human serum. Note the strongly positive signals on filaments that extruded from the germinated spores. (b) Positive results obtained by a 1 : 400 dilution from a symptomatic rabbit with natural *E. cuniculi* infection. Note the positive signals on the spore wall and the filament. Bars, 10 μm.

Culture supernatant containing MAb2 strongly reacted with a band at 52 kDa (Figure 2; strip P1). A serum from a naturally infected rabbit generated IgM antibody-positive multibands between 28 and 96 kDa, and also a few bands around 19 kDa (Figure 2; strip P2). However, the rabbit serum did not show any reduced influence in IgM antibody-binding of the 52-kDa band, even after NaOH treatment (Figure 2; strip P3).

Reactivities of ConA and mouse monoclonal antibody on 1-D blots before and after NaOH treatment

When untreated 1-D blots were used, ConA was the only one of seven lectins that revealed clearly positive binding to

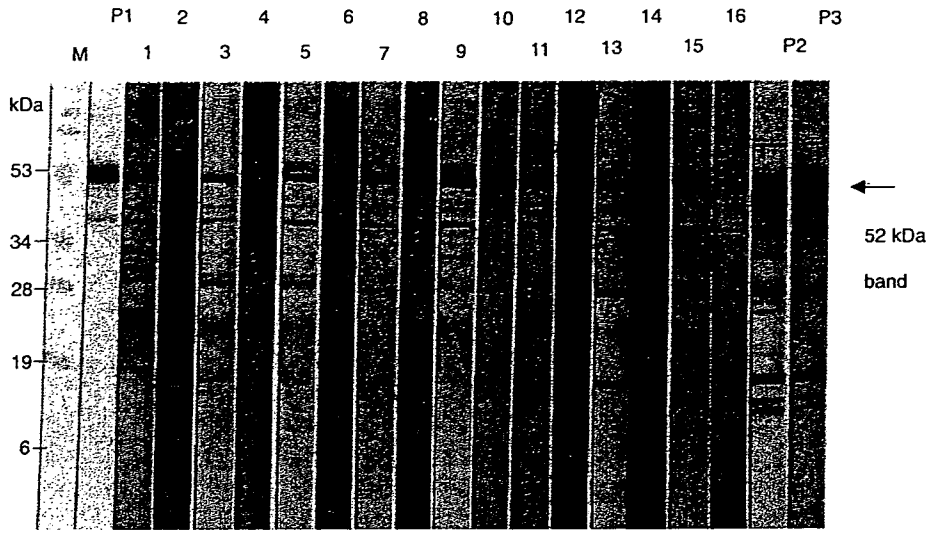

Figure 2 Binding profiles of human sera with anti-PT IgM antibody activities. *Encephalitozoon cuniculi* spore antigens were fractionated by 1-D PAGE and transferred to a PVDF membrane. Blotted strips before and after NaOH treatment were prepared and allowed to react with human serum samples followed by an anti-human IgM (μ-chain specific)-ALP conjugate. Odd-numbered strips and the P1- and P2-labelled strips were untreated, but even-numbered strips and the P3-labelled strip were treated with NaOH. Strips were reacted with each serum sample in pairs, starting from no. 1. M is a strip for markers of molecular weight (Prestained SDS-PAGE standards, Bio-Rad); P1 is a strip that reacted with MAb2; P2 and P3 are strips that reacted with a rabbit serum.

a 52-kDa band (data not shown). However, ConA did not bind at all to 1-D blots treated with NaOH (Figure 3; strip 2).

As seen on strip P1 in Figure 2 and strip 3 in Figure 3, MAb2 bound to the 52-kDa band on 1-D blots untreated with NaOH. However, MAb2-binding was not influenced by NaOH treatment at all (Figure 3; strip 4).

The location of the ConA-stained band on blotted strips was consistent with those bands detected by the monoclonal antibody (Figure 3). However, the band stained with ConA was always slightly thinner than bands detected by MAb2, suggesting that the PTP1 may be a mixture of different glycosylated and unglycosylated forms, which is likely to be slightly polydisperse in electrophoresis.

Identification of some proteins immunoreactive for human sera on 2-D blots

Eleven protein spots on a 2-D blot of *E. cuniculi* antigens were identified (Figure 4a, Table 1). Two of these spots, nos 1 and 2, had the same molecular size but different isoelectric points; these were identified as *E. cuniculi* polar tube protein (PTP), because both structures contained the peptide sequence ATALXSNAYGLTPGQQGMAQ by N-terminal amino acid sequencing. This has 90% sequence homology with the peptide sequence ATALCNAYGLTPGQQGMAQ of *E. cuniculi* genotype 1 (GenBank Accession No. AF310677) and was identified as PTP1 of *E. cuniculi* (SWISS-PRT

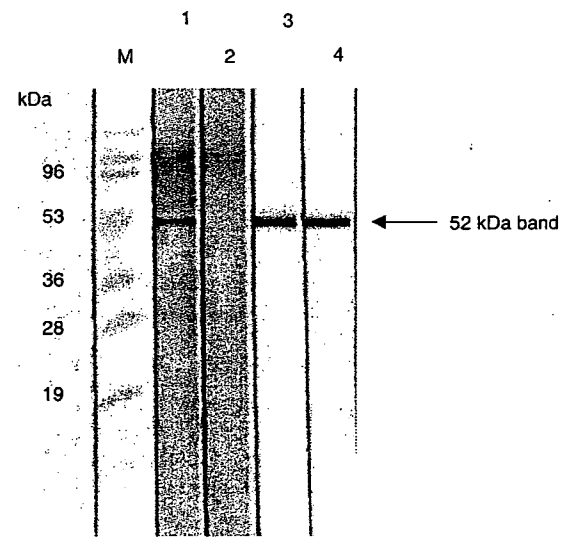

Figure 3 Binding profiles of ConA lectin and monoclonal antibody (MAb2) on 1-D blots. *Encephalitozoon cuniculi* spore antigens were fractionated by 1-D PAGE and transferred to a PVDF membrane. Blotted strips before and after NaOH treatment were prepared and allowed to react with ConA lectin and monoclonal antibody (MAb2). Odd-numbered strips were untreated, but even-numbered strips were treated with NaOH. Strip nos 1 and 2 and strip nos 3 and 4 were reacted with ConA and MAb2, respectively. M is a strip for markers of molecular weight (Prestained SDS-PAGE, Bio-Rad).

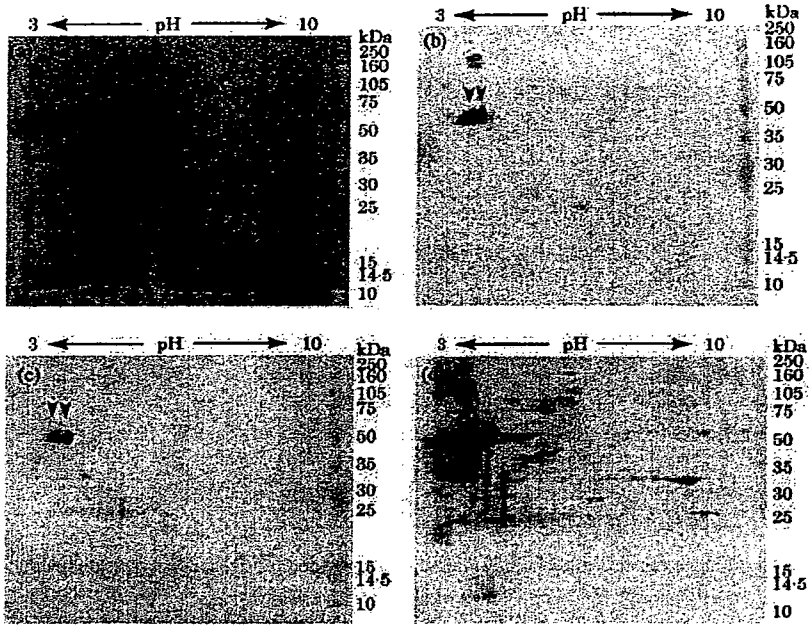

Figure 4 2-D immunoblot analysis. *Encephalitozoon cuniculi* spore antigens were fractionated by 2-D PAGE and transferred to PVDF membranes. (a) BODIPY FL-X staining: a blotted membrane is stained with the dye. Proteins extracted from 11 dye-stained spots (circles) identified by sequence analysis. (b–d) Immunostaining: blotted membranes incubated with H-168 serum (b), H-197 serum (c) and PRS (d). In the blotted membranes incubated with human sera (H-168 and H-197) containing anti-PT IgM antibodies, note the two acidic proteins (arrowheads) predominantly immunostained at 52 kDa; these proteins correspond to PTP1 spots capable of being stained with BODIPY FL-X, as seen in Figure 4(a).

Table 1 Human sera-immunoreactive spots in *E. cuniculi* identified by N-terminal amino acid sequencing (NTAAS) and LC-MS/MS

Spot no.	Protein	Accession no. (Swiss-Prot, NCBI)	Sequence coverage (%)	Method of identification	Immunoreactivity[a] with 168	197	PRS
1	Polar tube protein 1	sp. PTP1ENCCU	–	NTAAS	3+	3+	4+
2	Polar tube protein 1	sp. PTP1ENCCU	–	NTAAS	3+	3+	4+
3	Polar tube protein 2	gi: 19074274	21·3	LC-MS/MS	1+	0	2+
4	Translation elongation factor 1α	gi: 19074188	36·44	LC-MS/MS	0	0	1+
5	Spore wall protein 1	gi: 19074777	9·78	LC-MS/MS	0	0	2+
6	Hypothetical protein	gi: 19173268	42·86	LC-MS/MS	0	0	1+
7	Zinc finger protein	gi: 19074227	25·81	LC-MS/MS	1+	±	0
8	Similarity to HSP 70-related protein	gi: 19073931	29·55	LC-MS/MS	±	0	±
9	Heat shock-related 70 kDa protein	gi: 19173012	23·13	LC-MS/MS	0	0	±
10[b]	Phosphomannomutase	gi: 19173562	24·22	LC-MS/MS	0	0	0
11	6S proteasome ζ chain	gi: 19173680	17·67	LC-MS/MS	0	0	1+

[a]Immunoreactivity was examined by 2-D immunoblotting using human sera (H-168 and H-197) and rabbit sera (PRS – a pool of infected rabbit sera). The resultant intensity of each spot is scored as 0, ±, 1+, 2+, 3+ or 4+ (0, negative; ±, ambiguous; 1+ to 4+, graded positiveness). PRS was used as a positive control for 2-D immunoblot analysis.
[b]Spot no. 10 seems not to react with either human or rabbit samples, but was identified as a nonimmunogenic protein in this study.

database: PTP1ENCCU). This finding makes it clear that the 52-kDa PTP1 has more than one isoform.

H-168 and H-197 sera predominantly reacted with some spots that corresponded to PTP1 at 52 kDa (Figure 4b,c). These sera were examined as representative human sera with anti-PT IgM activities. H-168 serum also reacted with other protein spots, such as PTP2 and zinc finger protein (Figure 4b, Table 1). Such a positive reaction to zinc finger protein was not generated by a pool of sera from 11 naturally infected rabbits (PRS; Table 1).

When IgG antibodies in PRS were used as a positive control for 2-D immunoblot analysis, they reacted with spots that corresponded to PTP1, PTP2, spore wall protein 1, translation elongation factor 1α, hypothetical protein and 6S proteasome ζ chain in decreasing order of strength, as identified by LC-MS/MS analysis (Figure 4d, Table 1).

However, the rabbit IgG antibodies reacted very weakly with spots that corresponded to heat shock-related 70-kDa proteins (HSP70) and a protein with similarity to HSP70-related protein (Figure 4d, Table 1). Although a zinc finger protein and phosphomannomutase were also identified by LC-MS/MS analysis (Figure 4a), the corresponding spots were negative for rabbit IgG antibodies (Figure 4d, Table 1). IgG antibodies in a pool of 11 normal rabbit sera did not react with 2-D blots (data not shown).

Culture supernatant containing monoclonal antibody MAb2 reacted strongly with some spots of PTP1 at 52 kDa (data not shown).

DISCUSSION

All of the members of Microsporidia possess a unique, highly specialized structure, the PT, which is an organelle for invasion (15). *Encephalitozoon cuniculi* PT consists of three proteins: PTP1, PTP2 and PTP3 (16). The PTP1 is the major component of the PT and it is modified by O-linked mannose residues to which ConA binds (17).

In respect to antibodies against *Encephalitozoon* PT in immunocompetent persons, it has been reported that anti-*E. intestinalis* PT was demonstrated in 8% of Dutch blood donors and 5% of pregnant French women (18). Further study has demonstrated that carbohydrate moieties of the microsporidian PTPs are targeted by IgG in immunocompetent individuals (19). On the other hand, our study clearly indicates that the major activities of human anti-PT IgM antibodies are predominantly towards *E. cuniculi* PTP1, which is an acidic protein with an apparent molecular weight of 52 kDa in 2-D immunoblot analysis (Figure 4). Also, two chemically different antigenic sites can be found on the 52-kDa band in 1-D immunoblot analysis (Figure 2): proteinic determinant and saccharic determinant, as discussed below. In addition, although other few protein spots, such as PTP2 and zinc finger protein, weakly reacted with H-168 serum by 2-D immunoblotting, they did not appear to be effectively antigenic as compared to PTP1 (Table 1).

To analyse immunoreactivity of human anti-PT IgM with two different determinants, we used NaOH treatment capable of removing glycoepitopes from blotted antigens. Xu *et al.* (17) employed blots treated with 0·1 N NaOH at 50°C for 40 min to eliminate ConA binding to *E. hellem* PTP1. In our case, ConA binding to *E. cuniculi* PTP1 blotted onto a PVDF membrane was successfully eliminated by treating the blots with 0·05 M NaOH at 40°C for 16 h, conditions that were established by Duk *et al.* (13).

From the reactions of anti-PT IgM to the 52-kDa band after NaOH treatment, we could roughly group human sera into three categories when examined by 1-D immunoblotting: sera showing a completely negative profile; sera with a positive profile that was unmodified by NaOH treatment; and sera indicating a significantly reduced profile (Figure 2). Sera showing completely negative profiles are interpreted to have reacted with only a ConA-reactive determinant of PTP1 (Figure 2; strips 1–4). On the other hand, sera with a positive profile that was unmodified by NaOH treatment are interpreted to have reacted with only a proteinic determinant (Figure 2; strips 5–10). Interestingly, 41·3% (10/24) of the examined human serum samples belonged to the group with a significantly reduced profile. It was obvious that the significant reduction in binding after NaOH treatment resulted from the removal of the ConA-reactive determinant (Figure 2; strips 11–16), suggesting that this type of anti-PT IgM can recognize the saccharic determinant as well as the proteinic determinant. Thus, human anti-PT IgM could recognize the two determinants alone or in a pair, depending on serum used.

In a previous study (10) and also in this study, we confirmed that representative human sera with anti-PT IgM (H-168 and H-197) strongly immunostained the outer surface of filaments extruded from spores (Figure 1a). Our monoclonal antibody (MAb2) that could immunostain extruded PTs by ELISA definitely recognized the 52-kDa band by 1-D immunoblotting (Figures 2 and 3) and the PTP1 spots by 2-D immunoblotting (data not shown). Monoclonal and/or polyclonal antibodies raised to the purified *Encephalitozoon* PTP1 demonstrated reactivity with PTs by immunofluorescence and immunogold electron microscopy (17), indicating the presence of glycoconjugates in the PT. It has been proposed that the lipophilic regions of the PTPs adhere to the filament membrane and that the hydrophilic regions are orientated into the aqueous extrasporal environment (20). Thus, human anti-PT IgM-reactive determinants (constituted of saccharic and proteinic determinants and located on PTP1s) would be concentrated on the outside of the PTP coated on the surface of extruded filaments.

Regarding the specificity of anti-PT IgM in human sera, a previous study revealed that they did not react with extruded filaments from germinated *E. hellem* or *E. intestinalis*, indicating that human anti-PT IgM is species-specific (10). This finding was not in disagreement with previous findings that human sera containing anti-*E. intestinalis* PT IgG antibody activity did not immunostain filaments extruded from *E. cuniculi* or its PTP1 (19). One may consider that there is a cross-reactive relationship between microsporidian spores and fungal spores, because Microsporidia are phylogenetically related to fungi (21). However, apart from saccharic determinants, using an enzyme-linked immunosorbent assay, we found that MAb2 specific for *E. cuniculi* PTP1 did not cross-react with Laemmli sample buffer-extracted soluble antigens from the following fungi: *Candida albicans*, *Fusarium*

Journal compilation © 2007 Blackwell Publishing Ltd, *Parasite Immunology*, **30**, 13–21

moniliforme, *Eurotium*, *Aspergillus fumigatus*, *Curvularis*, *Aureobasidium pullulans*, *Trichoderma* sp., *Chaetomium globosum* and *Rhizopus stolonifer* (data not shown).

In respect to the specific human immune responses to the *E. cuniculi* infection, anti-spore wall IgG was observed to precede anti-PT IgG (7). Strong antigenicity and immunogenicity of *E. cuniculi* PTP1 have also been reported (20). However, most of our subjects were negative for anti-spore wall IgM and IgG, as noted previously (10). Moreover, anti-PT IgG antibodies were not detectable in most of our subjects (10). Therefore, these subjects may have been exposed to *E. cuniculi* spores, but showed little secondary immune response to their exposure. There is still the possibility that such IgM antibodies are cross-reactive antibodies produced by fungal infections, since the primary response usually is of low specificity. In these regards, further work needs to be done.

Apart from some extremely rare situations, it is most unlikely that microsporidiosis is provoked by *E. cuniculi* in immunocompetent persons (2,4,8). Considering that almost all human encephalitozoonosis cases occurred in immunocompromised patients (2,4–6), one can speculate that protective immunity plays a very important role against *E. cuniculi* infection. We previously showed that the rate of positivity for anti-PT IgM antibodies was significantly higher among healthy people than among HIV-positive persons, such that the CD4 cell level greatly affected the detection of anti-PT IgM antibodies (10). It should be emphasized that human microsporidiosis is predominantly associated with $CD4^+$ T cell deficiency (8,22). A recent report on intraocular microsporidiosis in a patient with idiopathic $CD4^+$ T-lymphocytopenia proves the infectivity of *E. cuniculi* for immunodeficient humans (23).

In a model of PT discharge, it has been thought that unpolymerized PTP is released from the PT core and polymerizes on the outside of the membrane scaffolding as it is being everted (20). If circulating anti-PT IgM antibodies react with these unpolymerized and polymerized PTPs, resultant antigen–antibody complexes may block the formation of PTs, thus preventing the PT from penetrating a host cell. However, as in other human opportunistic protozoal infections, microsporidian-specific antibodies alone may not be protective (22). In humans, cell-mediated immunity is said to be critical for protection against microsporidian organisms (22). More recently, Sak *et al.* (24) demonstrated that humoral antibodies enhance the protective effect of $CD4^+$ T lymphocytes using SCID mice perorally infected with *E. cuniculi*, suggesting that the humoral part of the immune system may contribute to the defence against microsporidial infection. Further studies on human anti-PT IgM need to be performed from the perspective of protective immunity.

ACKNOWLEDGEMENTS

The authors appreciate the assistance of Shigeru Miwa (Immunobion, LTD., Sapporo, Japan) who contributed by producing the specific monoclonal antibody, MAb2. We also thank Tokiko Asakura for her assistance with the serological testing and cell culture.

This work was supported by Grant-in-Aid no. 16390177 from the Ministry of Education, Science, Sports and Culture of Japan.

REFERENCES

1 Canning EU & Varva J. Phylum Microsporidia. In Lee JJ, Leedale GF & Bradbury P (eds): *The Illustrated Guide to the Protozoa*, 2nd edn. Lawrence, KS, USA, Society of Protozoologists, 2000: 39–126.
2 Mathis A, Weber R & Deplazes P. Zoonotic potential of the Microsporidia. *Clin Microbiol Rev* 2005; **18**: 423–445.
3 Didier ES, Stovall ME, Green LC, Brindley PJ, Sestak K & Didier PJ. Epidemiology of microsporidiosis: sources and modes of transmission. *Vet Parasitol* 2004; **126**: 145–166.
4 Weber R, Schwartz DA & Deplazes P. Laboratory diagnosis of microsporidiosis. In Wittner M & Weiss LM (eds): *The Microsporidia and Microsporidiosis*. Washington, DC, ASM Press, 1999: 315–362.
5 Mohindra AR, Lee MW, Visvesvara G, *et al.* Disseminated microsporidiosis in a renal transplant recipient. *Transplant Infect Dis* 2002; **4**: 102–107.
6 Gamboa-Dominguez A, De Anda J, Donis J, Ruiz-Maza F, Visvesvara GS & Diliz H. Disseminated *Encephalitozoon cuniculi* infection in a Mexican kidney transplant recipient. *Transplantation* 2003; **75**: 1898–1900.
7 van Gool T, Biderre C, Delbac F, Wentink-Bonnema E, Peek R & Vivares CP. Serodiagnostic studies in an immunocompetent individual infected with *Encephalitozoon cuniculi*. *J Infect Dis* 2004; **189**: 2243–2249.
8 Bryan RT. Microsporidiosis as an AIDS-related opportunistic infection. *Clin Infect Dis* 1995; **21** (Suppl. 1): S62–S65.
9 Franzen C & Muller A. Microsporidiosis: human disease and diagnosis. *Microbes Infect* 2001; **3**: 389–400.
10 Omura M, Furuya K, Kudo S, Sugiura W & Azuma H. Detecting immunoglobulin M antibodies against microsporidian *Encephalitozoon cuniculi* polar tubes in sera from healthy and human immunodeficiency virus-infected persons in Japan. *Clin Vaccine Immunol* 2007; **14**: 168–172.
11 Asakura T, Nakamura S, Ohta M, Une Y & Furuya K. Genetically unique microsporidian *Encephalitozoon cuniculi* strain type III isolated from squirrel monkeys. *Parasitol Int* 2006; **55**: 159–162.
12 Galfre G, Howe SC, Milstein C, Butcher GW & Howard JC. Antibodies to major histocompatibility antigens produced by hybrid cell lines. *Nature* 1977; **266**: 550–552.
13 Duk M, Ugorski M & Lisowska E. β-elimination of *O*-glycans from glycoproteins transferred to immobilon P membranes: method and some applications. *Anal Biochem* 1997; **253**: 98–102.
14 Hellman U, Wernstedt C, Gonez J & Heldin CH. Improvement of an 'In-Gel' digestion procedure for the micropreparation of internal protein fragments for amino acid sequencing. *Anal Biochem* 1995; **224**: 451–455.

